Environmental Science: Atmospheres

ROYAL SOCIETY OF CHEMISTRY

PAPER

View Article Online
View Journal | View Issue

Open Access Article. Published on 23 December 2024. Downloaded on 11/2/2025 12:57:08 AM.
This article is licensed under a Creative Commons Attribution-NonCommercial 3.0 Unported Licence.

Check for updates

Cite this: *Environ. Sci.: Atmos.*, 2025, **5**, 220

# Assessing conditions favoring the survival of African dust-borne microorganisms during long-range transport across the tropical Atlantic†

Ali Hossein Mardi,[a] Miguel Ricardo A. Hilario,[b] Regina Hanlon,[c] Cristina González Martín,[d] David Schmale,[c] Armin Sorooshian[be] and Hosein Foroutan*[a]

Received 1st July 2024
Accepted 20th December 2024

DOI: 10.1039/d4ea00093e

rsc.li/esatmospheres

Forward trajectories of trans-Atlantic dust plumes were studied over a 14 year period (N ~500 000) with a focus on ambient meteorological conditions affecting the survivability of the microorganisms co-transported with dust. Major dust transport patterns that emerged from the ensemble of trajectories closely follow the established seasonal transport patterns of African dust over the tropical Atlantic Ocean: summer transport (June–August) reaching the southeastern US and the Caribbean at an average altitude of 1600 m and winter transport (December–February) reaching the Amazon basin at around 660 m. Summer trajectories take on average 270 hours to cross the Atlantic, while winter ones take 239 hours. A higher diversity is expected in microorganisms co-transported to the Amazon due to the higher diversity in contributing dust emission sources. Analysis of meteorological conditions along the trajectories indicate more favorable conditions for microorganism survival reaching the Amazon. During the winter and for Amazon trajectories, lower mean solar radiation flux of 294 W $m^{-2}$ and mean relative humidity levels at around 61% are observed as compared to averages of 370 W $m^{-2}$ solar radiation and 45% relative humidity for summer trajectories entering the Caribbean basin. Nevertheless, 14% of winter trajectories (4664 out of 32 352) reaching the Amazon basin face intense precipitation, potentially removing microorganisms, as compared to 8% of trajectories (2540 out of 31 826) entering the Caribbean basin during the summer. These findings have important implications for the survivability of microorganisms in trans-Atlantic dust plumes and their potential for major incursion events at receptor regions.

### Environmental significance

Annually, substantial portions of dust aerosols originating from northern Africa travel across the Atlantic Ocean through the atmosphere and impact areas as far as U.S. southeast, the Caribbean, and the Amazon. A lesser studied aspect of this phenomenon is the co-transport of a wide range of microorganisms onboard the dust aerosols. We studied the seasonal variations in travel path, altitude, and ambient meteorological conditions along dust transport trajectories across the Atlantic Ocean focusing on transport conditions impacting the concentration, diversity, and longevity of transported microorganisms. Results suggest a more suitable condition for the survivability of microorganisms reaching the Amazon during the winter; however, a greater portion of trajectories face intense precipitation and potential removal during that time of the year.

## 1. Introduction

The most abundant type of aerosol in the atmosphere by mass is dust[1,2] of which the greatest portion is emitted from the surface of desertified regions where evaporation exceeds the mean annual precipitation.[3,4] Deserts of North Africa, including the Sahara and Sahel regions are one of the world's most prominent dust sources[5–7] with the greatest emission contributed by the Sahel area.[8] A great portion of this annual emission traverses the Atlantic Ocean and ultimately reach distant downwind regions. Dust is continually emitted from African sources throughout the entire year, and these emissions exhibit

[a]Department of Civil and Environmental Engineering, Virginia Tech, Blacksburg, Virginia, USA. E-mail: hosein@vt.edu
[b]Department of Hydrology and Atmospheric Sciences, University of Arizona, Tucson, Arizona, USA
[c]School of Plant and Environmental Sciences, Virginia Tech, Blacksburg, Virginia, USA
[d]Instituto Universitario de Enfermedades Tropicales y Salud Pública de Canarias, Universidad de La Laguna, San Cristóbal de La Laguna, Spain
[e]Department of Chemical and Environmental Engineering, University of Arizona, Tucson, Arizona, USA

† Electronic supplementary information (ESI) available. See DOI: https://doi.org/10.1039/d4ea00093e


© 2025 The Author(s). Published by the Royal Society of Chemistry

Open Access Article. Published on 23 December 2024. Downloaded on 11/2/2025 12:57:08 AM.
This article is licensed under a Creative Commons Attribution-NonCommercial 3.0 Unported Licence.

a correlation with the westward component of the 700 mb (~2700 m) wind above the African continent.[9,10] From time to time, there are sporadic and intense dust plumes that pulse through the Atlantic Ocean in intermittent waves and increase the concentration of particulate matter (PM) far above the seasonal backgrounds at downwind regions.[11]

Dust emissions across North Africa are not uniform, with certain regions exhibiting higher emission rates. For instance, the Bodélé depression in Chad is recognized as the world's largest source of dust emissions.[12–14] Additionally, the western regions of North Africa, situated between Mali and Mauritania, are another significant aeolian dust source.[14] Further research suggests that the spatial variations in the location of major dust sources follow a seasonal pattern. Ashpole and Washington[15] applied a neural network-based classification scheme on daily dust occurrence and specified two distinct regions as major sources of emission over North African arid regions. One region located where Algeria, Mali, and Niger meet with highest emission activity from December to February and emissions progressing toward the Mali and Algerian border from June to August. A similar seasonal variation pattern in the sources of dust emissions is also observed through remote sensing data from the Cloud-Aerosol Lidar and Infrared Pathfinder Satellite Observation (CALIPSO)[16,17] and Meteosat Second Generation (MSG), utilizing the 8.7, 10.8, and 12.0 mm wavelength channels.[18] These observations indicate that northwestern sources are most active during the hot and dry season (June to August) and during the boreal winter, the dust emissions shift closer to the equatorial regions and over the Bodélé depression.

In winter, synoptic scale processes play a significant role in driving episodic and intense emissions, primarily concentrated in the lower portion of the atmosphere,[19] often within or near the marine boundary layer.[20] Observations of the seasonal average dust layer height using CALIPSO indicate that, during winter emissions, the average top height is approximately 2 kilometers along a meridional trajectory.[17,21] In the summertime, dust emissions exhibit a greater variety of sources and mechanisms, often resulting in a vertically extended dust layer that can reach heights ranging from 5 to 7 kilometers.[22] This summer-time African dust layer is commonly referred to as the Saharan dust layer, known for its unique characteristics such as its extended altitude and significantly lower moisture content compared to the adjacent air layers.[23] Summertime dust emissions tend to ascend to higher atmospheric levels as they move towards the cooler air outside the western boundary of the Sahara.[19,20] Dust aerosols travel path across the Atlantic is mainly governed by the seasonal variations in the location of the inter tropical convergence zone (ITCZ), which limits the southern extent the plumes can reach.[7,21]

Microorganisms thrive in a variety of aquatic and terrestrial environments and knowledge of their sources and potential contribution to the global climate budget has received considerable attention.[24–26] The atmosphere is teeming with microscopic life[27,28] and dust aerosols are well documented as a vessel for carrying microorganisms. The direct link between dust aerosols and transport of microorganisms is depicted in the form of an increase in the number of Colony Forming Units (CFU) in samples collected during the dust events as compared to the background conditions[29] (and references therein). Notes of airborne transport of microorganisms are dated back to early days of discovering microorganisms.[30,31] Several cases of modern crop plant diseases are documented to be transported across the continents *via* aerial dispersion of spores of plant pathogenic fungi.[32] Microorganisms may be transported as individual cells (*e.g.* spores), in clusters (*e.g.*, conidiophores), and/or attached to dust particles and previous studies of atmospheric dust have revealed the presence of diverse bacterial communities.[33–36]

Specific to the arid North African regions of Sahara and Sahel, three main phyla of Actinobacteria, Firmicutes, and Proteobacteria are detected as the most abundant types in sands of Bodélé depression and surrounding regions.[35] Across four field campaigns conducted in the Yucatán Peninsula, Mexico, the same three bacterial phyla consistently dominate the culturable bacterium samples where terrestrial microbiota were predominant and African dust deposition is noted as a contributing factor.[37] During episodes of severe African dust impact on the Caribbean, the number of cultivable microorganisms is reported to increases by a factor of three compared to clear atmospheric conditions and the majority of the detected microbial isolates are predominantly associated with soil and plant species.[38] Additionally, traces of atmospheric dust have been found in the most remote areas of the world with estimated travel time-scales at around 13 days.[39–41] Consequently, microorganisms traveling with dust have the potential to be transported around the world and impact the atmospheric microbiome of the receptor regions[42–44] by transport of high-threat or invasive pathogens.[35,38,45,46]

Presence of African dust over Caribbean and Amazon is an established fact. One of the earliest observations of African dust long-range transport across the Atlantic is dated back to 1956, which at the time was found surprising, given the 7–10 days duration of travel and various deposition factors impacting the dust plumes.[47] This finding was later confirmed by isotopic analysis on numerous dust samples collected over Caribbean basin and Amazon[48,49] and by study of the chemical composition of collected aerosols.[22,50] Though trans-Atlantic transport of dust has been the subject of a considerable amount of research[51] (and references therein), the long-range co-transport of microorganisms and dust aerosols is one of the lesser studied aspects of this phenomenon.[52]

Several crucial parameters affect the composition and diversity of microorganisms found within dust aerosols, with the origin of the dust being a particularly significant one. Additionally, the location of the dust source can influence the size distribution of aerosolized dust particles, the duration of their travel, and the atmospheric conditions encountered by these dust aerosols[51,53] which motivates the need for the analysis of dust source locations. Nevertheless, it is challenging to identify the exact source of emission for each receptor region based on current remote sensing or *in situ* methods.[14,51] Moreover, as dust particles passively travel *via* global circulation, the amount of transported dust, the regions they reach, and the conditions they experience along the way are driven mainly by

Open Access Article. Published on 23 December 2024. Downloaded on 11/2/2025 12:57:08 AM. This article is licensed under a Creative Commons Attribution-NonCommercial 3.0 Unported Licence.

prevailing circulation regimes from the emission point up to the receptor region.[54] These challenges emphasize the need for a novel approach that could overcome some of the existing limitations in detecting the exact origin of dust and ambient meteorological conditions endured by co-transported microorganisms along the way. To overcome these challenges, we examined seasonal trends in atmospheric trajectories of trans-Atlantic dust over a period of 14 years (2008–2021) and their implication for microorganisms' transport. We hypothesize that seasonal trends observed in dust emission sources, travel path, and ambient meteorological conditions along these trajectories will lead to distinct environmental conditions that can benefit the co-transport of different taxa of microorganisms, depending on the season, contributing sources, and the receptor region. To test this hypothesis, we combined a dust emission scheme and forward trajectory analysis to characterize ambient conditions along each dust transport trajectory from the point of emission until it reached our defined receptor regions. The specific objectives of this study were to (1) connect dust source and receptor regions across the Atlantic Ocean, (2) report on the seasonal trends observed in dust trajectories and ambient conditions along the way with a focus on the implications for viability and diversity of the microorganisms. Through this analysis, we plan on setting a basis for future studies of dust and microorganism samples collected across the Atlantic. We aim to employ a comprehensive approach that considers every arid region of the North African continent located at topographically low regions as a potential source of dust emission. After locating major seasonal sources of dust, we report on the trajectories initiated from North African sources that reach two receptor regions located on the western side of the Atlantic Ocean (US-CARIB and AMZN). We report on the spatial and vertical distribution of these trajectories along with transport duration through different seasons to depict a seasonally resolved demonstration of dust travel across the Atlantic. We then compare these results with literature and evaluate their compatibility as an evaluation to our method and outputs. Next, we discuss the amount of dust emission associated with these trajectories to isolate emission areas with relative importance for defined receptor regions. In the final section, we discuss the average meteorological condition experienced by the majority of the dust trajectories across the Atlantic and its potential influence on the type, concentration, and diversity of co-transported microorganisms.

## 2. Data and method

### 2.1. Dust emission sources

NASA Modern-Era Retrospective analysis for Research and Applications, Version 2 (MERRA-2)[55] is a continuation of the modern satellite era (1980 onward) atmospheric reanalysis run and managed by the NASA Global Modeling and Assimilation Office (GMAO). The MERRA-2 system incorporates more contemporary datasets not available to the original MERRA reanalysis dataset with an improved meteorological observing system. One of the greatest advantages of MERRA-2 is having analyzed aerosol fields that can be used as an input in analysis of the interaction between aerosols and regional climate.

In MERRA-2, dust mass mixing ratios are simulated with a radiatively coupled version of the Goddard Chemistry, Aerosol, Radiation, and Transport model (GOCART)[56] for five non-interacting size bins. Dust emission values are wind driven for each size bin and calculated based on the parameterization provided by Marticorena and Bergametti.[57] Dust emission is derived based on a map of potential dust source locations, according to the observed co-location of large-scale topographic depressions and dust emitting regions first described by Ginoux *et al.*[56] In their model, the emission source functions are based on the colocation of TOMS AI hotspots detected by Prospero *et al.*[12] and topographic depressions. The emission budget from these dust source regions was further evaluated by simulation of atmospheric dust through the GOCART model and comparison of the results with global observations of dust concentration at the surface level, different vertical levels, deposition at surface, optical thickness and size distribution. Comparisons demonstrate levels of success in reproduction of distribution patterns of dust at the global scale by considering emissions from the mentioned hotspot regions. This scheme has also demonstrated capabilities in capturing the seasonal patterns of variations in surface concentration and optical thickness in dusty regions.[56] Nevertheless, it is important to note that the MERRA-2 dust emission scheme relies solely on model estimation and does not incorporate data assimilation. Recent *in situ* measurements have revealed a discrepancy in the observed size distribution of dust plumes, showing a notably higher abundance of dust aerosols with a diameter greater than 10 μm.[58] This discrepancy results in an overestimation of the emitted fraction of clay aerosols (<2 μm diameter) in global circulation models. This adjustment is made to match the radiative properties of dust plumes, which, in general, leads to an underestimation of the actual dust emission rate. Even though the MERRA-2 reanalysis data incorporate the deposition and hygroscopic growth of the aerosols after their emission, in this study we use the MERRA-2 dust emission scheme only to isolate the emission hotspots based on their long-term seasonal activity.

MERRA-2 hourly dust emission data were obtained for 2008–2021 (collection M2T1NXADG, DOI: **https://doi.org/10.5067/HM00OHQBHKTP**), in five different size bins (DUEM001–005, kg $m^{-2}$ $s^{-1}$) covering a dry radius range from 0.1–10.0 μm for an area in North Africa covering 12° N–38° N and 18° W–40° E (Fig. 1). Hourly emissions of different size bins were summed up for each day to create daily dust emission value maps with a spatial resolution of 0.5° × 0.625°. To obtain the seasonal dust emission hotspots, first the daily emissions of all days of that season were averaged to create a composite map of average seasonal emission. Next, a gamma distribution was fitted to the pixel values of each map and the $80^{th}$ percentile on the corresponding cumulative distribution function was selected as the threshold. On each map, the pixels with seasonal average values greater than the threshold obtained for that season were nominated as the seasonal dust emission hotspots. Finally, for each pixel of the nominated dust emission hotspots and during each day of that season, if

 © 2025 The Author(s). Published by the Royal Society of Chemistry

Open Access Article. Published on 23 December 2024. Downloaded on 11/2/2025 12:57:08 AM.
This article is licensed under a Creative Commons Attribution-NonCommercial 3.0 Unported Licence.

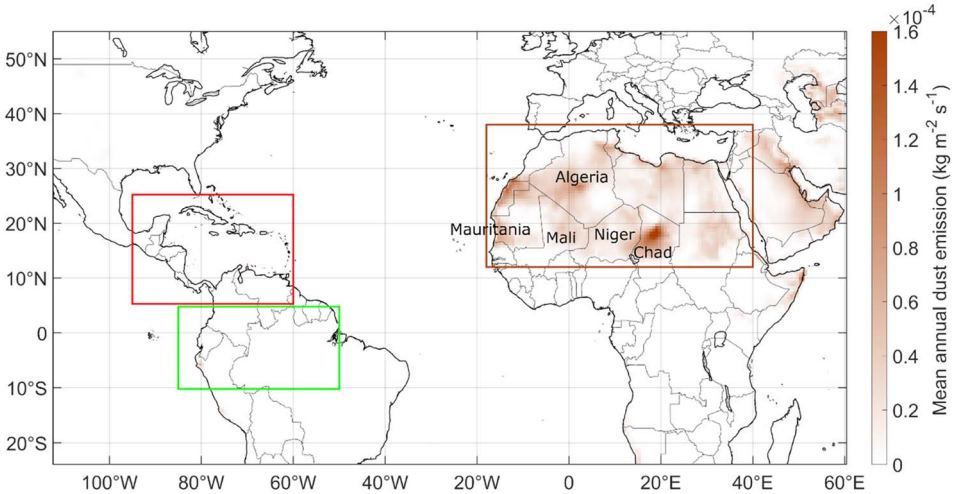


Fig. 1 The approximate boundaries of the study region. Two dust receptor regions are shown as US-CARIB (red rectangle) and AMZN (green rectangle). The MERRA-2 mean annual dust emission values are projected and represented by the color bar. The brown rectangle is where the HYSPLIT forward trajectories are initiated following observed dust emission activities.

the daily dust emission value was greater than 85$^{th}$ percentile of total daily emission values, that day was selected as a significant dust emission day for that pixel. Hereafter, we refer to these incidents as dust emission activities. Both 80$^{th}$ and 85$^{th}$ percentile thresholds were tuned to cover the majority of seasonal dust emission areas and be inclusive of the majority of daily dust emission incidents yet, keep the total number of trajectories within our data processing capacities. Over the course of study, more than 500 000 pixels of dust emission activities were nominated by this method and provided as inputs to the trajectory analysis.

It is important to emphasize that this emission and transport scheme focuses specifically on extreme dust emissions. Regardless of the geographic receptor region, these intense episodes of African dust emissions hold significant importance as a few extreme dust events can contribute a substantial portion of the annual dust budget at the receptor region.[11] Moreover, these intense emission episodes have a higher likelihood of surviving the deposition mechanisms during their journey, thereby leaving a profound impact on the receptor regions. This impact can manifest in the form of increased mineral deposition[59,60] or microbial activity[29,61] (and references therein). Fiedler *et al.*[62] estimated that annually, 55% of African emissions occur within close proximity to geographic depressions, a number that can rise to 90% on a seasonal scale. This finding is relevant, given that these geographic depressions served as the foundation for identifying the hotspots in the present study. However, it is crucial to highlight that especially in regions near the emission sources, local standard emissions also constitute a large portion of total deposited dust, annually.

### 2.2. Dust atmospheric pathways

To track the dust emission activities and report on their endured condition along the trajectories, NOAA Hybrid Single-Particle Lagrangian Integrated Trajectory model (HYSPLIT) was used.[63–65] HYSPLIT single trajectory analysis has a proven record in studying the origin or transport of air parcels in the atmosphere. Neff and Bertler[66] used HYSPLIT forward trajectories to explore transport of dust from southern hemisphere sources to the Southern Ocean and Antarctica over a three decade span. In their analysis, they initiated 10-day forward trajectories from possible dust sources at 100 m altitude above ground level using reanalysis meteorology fields provided by the National Centers for Environmental Prediction/National Center for Atmospheric Research (NCEP/NCAR). There cannot be a preset initial condition for HYSPLIT trajectories as different studies might benefit from HYSPLIT trajectory modeling according to their specific research goals. One of the earliest of such studies was Swap *et al.*[67] who tracked a dust incident both from a location near Chad in forward mode and from a receptor region in Amazon, in backward mode. They analyzed a range of initiation altitudes ranging from 600 to 975 mb, equivalent approximately to 4500 to 600 m, respectively. They reported 700 mb (~2700 m) as the altitude with closest resemblance to aircraft *in situ* observations. As a part of a comprehensive analysis of Bodélé dust impact on the Amazon, Ben-Ami *et al.*[68] initiated a series of HYSPLIT forward trajectories from several locations over the Bodélé at 0, 500, and 1000 m above the ground level. They reported on trajectories reaching the Amazon in a period of 10–17 days and at an altitude of 1700 to 5000 m, which best represent the *in situ* and remote sensing retrievals of the studied dust plume. A similar study analyzed the seasonal climatology of HYSPLIT forward trajectories over lake Eyre in Australia for five levels, starting from surface to 5000 m above the ground level.[69] They used the NCEP/NCAR global reanalysis meteorological dataset with trajectories extended for up to 8 days. In an attempt to cluster arriving trajectories over rural and urban sites located at United Kingdom, Abdalmogith *et al.*[70] ran three-day backward HYSPLIT trajectories 6 hours apart using the NCEP meteorology files. It is inferred from the mentioned analyses that analysis with a focus on transport in the higher altitudes of the atmosphere select a higher initial altitude for trajectories, usually above the 600 m AGL.

Open Access Article. Published on 23 December 2024. Downloaded on 11/2/2025 12:57:08 AM.
This article is licensed under a Creative Commons Attribution-NonCommercial 3.0 Unported Licence.

Accordingly, for each pixel designated as a dust emission activity, we chose to start trajectories in forward mode from an altitude of 300 m above the ground level on a daily basis. This altitude was selected to minimize the risk of trajectories interfering with surface terrain and be inclusive of low altitude atmospheric transport scenarios. All of the trajectories were initiated at 00:00:00 UTC and run for 360 hours, equivalent to 15 days to assure that the majority of the trajectories reached the downwind receptor regions. Two receptor regions were defined in the downwind area (Fig. 1), one covering the southeast U.S. and Caribbean (5° N–25° N and 65° W–95° W, US-CARIB from now on) and the other covering parts of the Amazon (10° S–5° N and 50° W–85° W, AMZN from now on). The location and boundaries of the receptor region were defined based on the reported oscillation pattern of trans-Atlantic dust transport trajectories due to the seasonal variation of the ITCZ over the Atlantic Ocean.[7,19,21,51,71,72] Locations were selected to ensure they received the majority of westward trajectories originating from the North African arid areas. The NCEP/NCAR Reanalysis archived data were used for HYSPLIT runs with a spatial resolution of 2.5 degree of latitude and longitude on a global grid and with an output every 6 hours.[73] It should be noted that the resolution of the meteorology model powering the HYSPLIT trajectories have a great impact on model's ability to represent the dust transport over small distances, specifically over the Sahara. Given the spatial resolution, the model is expected to predict the direction at which the dust particles move, however, it would be challenging for the model to capture the fine-scale evolution of the dust plumes due to the coarse resolution. This would not be surprising because even models with finer spatial resolutions are still not capable of capturing the dynamic evolution of dust plumes at synoptic scales.[74] The top of the model was set at 10 km, and model vertical motion was based on the input meteorological data. The NCEP/NCAR Reanalysis archived data are available from 1948 onward; however, the dataset's ability to represent the real-world conditions increased considerably after 1970, due to increased number of observations provided as an input for the assimilation.[75] The meteorological parameters were also reported along the trajectories for further analysis.

To better capture the governing flow of the wind over the region of study, seasonal mean wind velocity and directions were obtained from the eastward and northward components of NCEP-NCAR Reanalysis 1 (ref. 73) and averaged over the area of study for two different pressure levels of 1000–850 mb and 850–650 mb. The averaging over the 1000–850 mb level would best represent the governing wind fields within the boundary layer and the 850–650 mb was selected to represent the flow of air in the free troposphere and adjacent to the top of atmospheric boundary layer. For this purpose, we used monthly mean values averaged from the NCEP initialized reanalysis which is calculated by temporal resolution of four times per day and a spatial resolution of 2.5 degree for 17 altitudinal pressure levels, covering 1000–10 mb.

The HYSPLIT forward trajectory analysis inherently comes with uncertainties, including but not limited to the coarse resolution of the meteorology files and long trajectory run time[65,76–78] (and references therein). For analysis of the archived data, these uncertainties can be categorized as physical errors, due to inaccurate representation of the space and time for the atmosphere, computational errors as a result of numerical inaccuracies, and measurement errors caused by misrepresentation of real-world conditions by meteorological data fields. It requires extensive knowledge of real-world atmospheric measurements to assess the extent of computational and measurements errors for the HYSPLIT model, which we believe is beyond the scope of the current study. However, by comparing backward trajectories initiated from the point each trajectory had entered receptor regions, a so-called forward/backward trajectory analysis is performed.[79] This evaluation was done for the select year of 2021 with an applied methodology similar to the one described by Freitag *et al.*,[80] where the start points of backward trajectories are compared to the end points of trajectories initiated from the end point of initial backward trajectories. For the purpose of current study, we compared the end point of backward trajectories initiated from the point each forward trajectory had entered each receptor region and run for the same duration of steps to the starting point of each corresponding forward trajectory. Additionally, we have averaged meteorological parameters such as RH, ambient temperature, and solar flux along these trajectories and compared them to the initial forward ones.

In addition to the uncertainties mentioned above, the embedded uncertainties in the dust emission scheme do not enable us to report on properties and fate of each individual dust emission trajectory with certainty and this approach lacks calculated consideration of dust deposition which makes the emissions reported to be the maximum possible. Nonetheless, through this approach, we aim to establish pathways from North African dust emission regions to receptor sides on the western side of the Atlantic by combining more than 500 000 trajectories over a period of 14 years, and gauge the uncertainty associated with the trajectory model[81] for the seasonal trends governing the majority of dust trajectories across the tropical mid-Atlantic. Of all dust trajectories sourced from North Africa, only westward trajectories that reach either one of receptor regions were isolated for further analysis. It is possible for a trajectory to impact more than one region and be counted for both. For a trajectory to impact a receptor region, the average altitude of trajectory inside that region must be below 5 km. This criterion is defined to neglect those trajectories that pass above the receptor regions at higher altitudes. An additional criterion has been defined to exclude trajectories that travel eastward, eventually reaching receptor regions from the opposite direction after circling the globe. To achieve this, the general direction of each trajectory is calculated by summing the trajectory longitudes for the initial 120 steps, which corresponds to one-third of the total trajectory duration. This calculated general direction represents the longitudinal position of each trajectory relative to its starting point. Trajectories that end up east of their initiation point after 120 steps are excluded from the analysis.

### 2.3. Meteorological parameters

For each forward trajectory, the mean downward solar radiation flux (W $m^{-2}$), ambient temperature (K), RH (%), and

 © 2025 The Author(s). Published by the Royal Society of Chemistry

Open Access Article. Published on 23 December 2024. Downloaded on 11/2/2025 12:57:08 AM. This article is licensed under a Creative Commons Attribution-NonCommercial 3.0 Unported Licence.

precipitation (mm $h^{-1}$) from NCEP/NCAR reanalysis were calculated for the duration of travel time from the emission point to the receptor region. In addition to the means, values were also integrated for the travel path to reflect the total impact perceived by each trajectory and account for differences in travel times. By multiplying the solar radiation flux by number of steps with an hour of duration for each step, total solar radiation dose (J $m^{-2}$) was calculated for each trajectory, similar to the methodology used by Kowalski.[82] For ambient temperature (and RH), we used an integration scheme as follows:

$$T_{\mathrm{amb,P}} = \left( \sum_{i=1}^{n} \frac{1}{T_{\mathrm{amb,i}}} \right) \times n \tag{1}$$

In eqn (1), $T_{\mathrm{amb,P}}$ is the path integrated value of $1/T_{\mathrm{amb}}$ over $n$ number of steps for each trajectory with the unit of h $K^{-1}$. The purpose behind integrating the inverted values of $T_{\mathrm{amb}}$ is to reach a higher integrated value for trajectories experiencing lower temperatures for a longer time. Similarly, $RH_{\mathrm{amb,P}}$ is calculated for the duration of each trajectory with a unit of h per percent RH and a higher number reflects a lower RH impacting the trajectories for a longer period of time.

## 3. Results and discussion

### 3.1. Forward trajectory analysis

Table 1 summarizes the number of trajectories reaching each receptor region during each season. From more than 500 000 dust associated trajectories emitted from the North Africa, 115 715 trajectories (23%) impacted either one of designated receptor regions. Each one of the receptor regions has received approximately half of the total trajectories with 68 564 and 56 113 trajectories reaching US-CARIB and AMZN, respectively. Together, these numbers add up to 124 677 trajectories which include 8962 trajectories that have impacted both sub-domains and are accounted for both. Selection of receptor regions, based on the seasonal oscillation of the cross Atlantic dust transport pathway can be the reason behind receiving approximately half of the trajectories at each region. This oscillation is mainly driven by the seasonal change of the latitudinal location of the ITCZ.[51]

The majority of the trajectories reached US-CARIB during June–August with an average latitude of 17.5° N, and AMZN during December–February with an average latitude of 9.6° N, which is also evident in Fig. 2 (panels a–h). Results obtained for both the seasonality and the transport pathways are consistent with previous reports on trans-Atlantic dust transport[51,83,84] (and references therein). Another notable difference among the receptor regions was the altitude at which the trajectories traveled before reaching each receptor region. As depicted in Fig. 2 (panels i–p), the summer trajectories reached higher levels of the free troposphere immediately after leaving the African continent at about 25° W with an average altitude of 1639 m for US-CARIB trajectories during the June–August season. In contrast, the winter trajectories reaching the AMZN traveled over a notably lower mean altitude of 663 m from December to February. The vertical structure of the frequency of trajectories captured by the model matches the frequency of dust observations from CALIOP measurements with seasonal maximums observed at 2 km during June–July, and below 1000 m during December–February.[7,16,17,20,21] Observations during the Puerto Rico Dust Experiment (PRIDE) in July 2000 confirmed the presence of dust inside the marine boundary layer in higher concentrations as compared to the Saharan air layer above[85] This is mentioned as a possibility for dust transport only occurring within the marine boundary layer;[86] however, it was observed during a different season. It is also denoted that for this geographic region, trajectories that are associated with a higher concentration of dust at the point of reception, travel at a lower median altitude,[86] which is in accordance with results from our modeling. This is also important as the interaction between the co-transported dust microbiome and ocean surface is one of the main drivers of variations in ocean surface microbial activity.[44,87] The different seasonal trajectory path and altitude have implications for longevity, concentration, and diversity of onboard microorganisms as it implies different mean temperatures, solar radiation dose, and RH are experienced by microorganisms.[88,89] More details of trajectories' seasonal mean path and altitude can be found in Table S1.†

Fig. 3 shows the seasonal histograms of travel duration for trajectories impacting each receptor region. On the histograms, a cut off is evident at 360 hours which is due to 360 steps duration chosen for forward trajectories. The existing limitation in the number of steps does not allow for a complete depiction of dust trajectories. Nevertheless, we believe that the selected number of steps allows capturing of the majority of dust trajectories that reach the receptor regions because the travel time at which the highest number of trajectories travel are captured with the current run time. We do not expect to see a new peak for travel times higher than fifteen days because the longest travel times mentioned for African dust carrying trajectories are in the order of fifteen days[51] and this was the basis for selecting the current number of steps. It should also be noted that trajectories with longer travel times have lower possibility for transporting viable cultures of microorganisms, due to having microorganisms exposed for a longer period of time to the extreme atmospheric environment.[90] Comparing peak seasons of December–February and June–August, summer time trajectories spend a longer period of time traveling before reaching the receptor regions, which implies a lower possibility for transporting viable microorganisms due to being exposed to the harsh atmospheric environment for a longer period of time. Longer transport times also increase the likelihood of dust

Table 1 The seasonal change in the number of trajectories that occurred during each defined seasonal range for the two sub-domains, the southeast United States and Caribbean (US-CARIB), and Amazon (AMZN)

| # Trajectories | Dec–Feb | Mar–May | Jun–Aug | Sept–Nov | Total |
|---|---|---|---|---|---|
| US-CARIB | 7839 | 9377 | 31 826 | 19 522 | 68 564 |
| AMZN | 32 352 | 11 883 | 3305 | 8573 | 56 113 |
| Total | 40 190 | 21 260 | 35 131 | 28 095 | 124 677 |

Open Access Article. Published on 23 December 2024. Downloaded on 11/2/2025 12:57:08 AM.
This article is licensed under a Creative Commons Attribution-NonCommercial 3.0 Unported Licence.

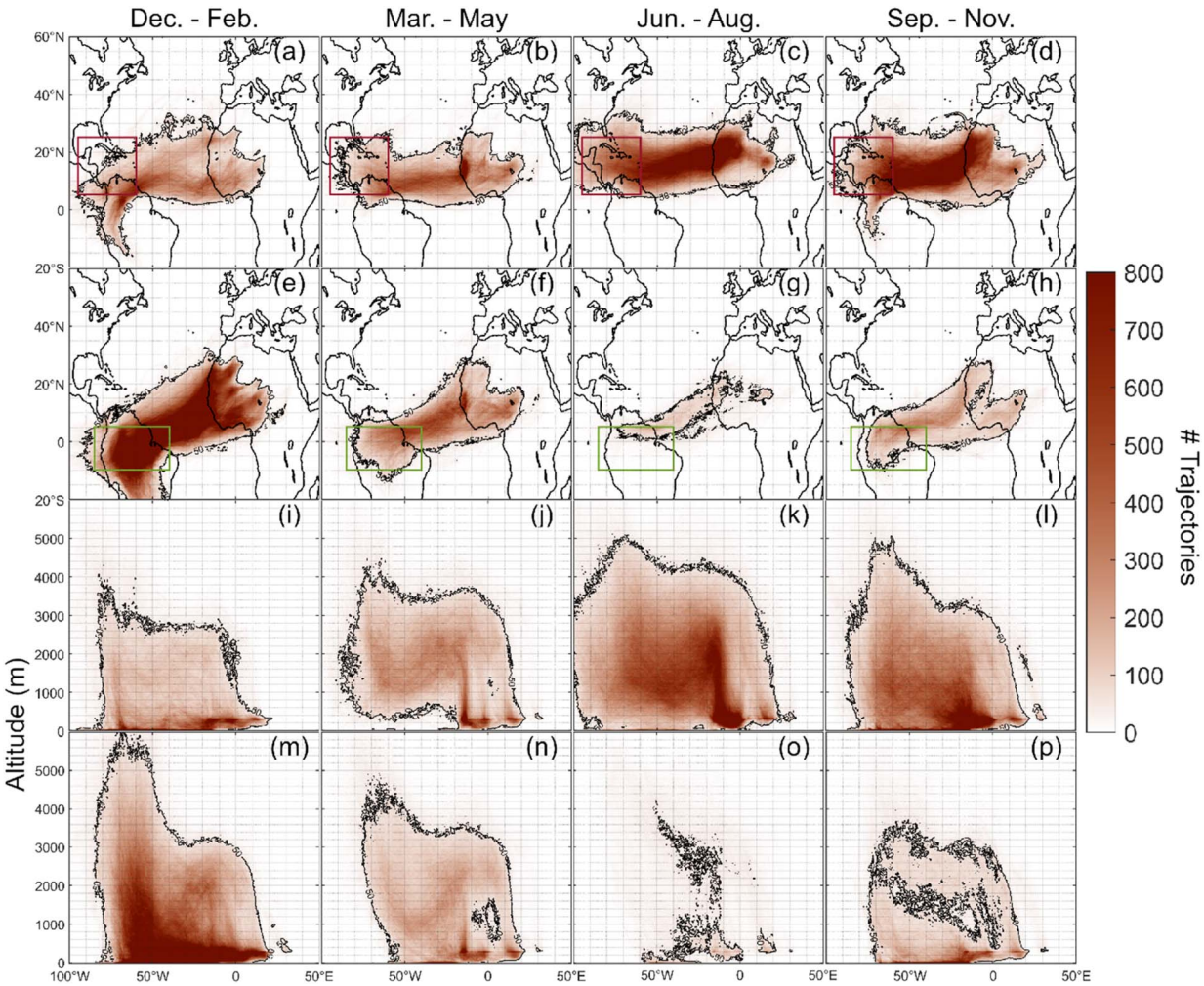


Fig. 2 Seasonal trajectory density maps for US-CARIB (a–d) and AMZN (e–h) receptor regions during December–February, March–May, June–August, and September–November. Seasonal density maps of the altitudes taken by trajectories from the point of emission until reaching US-CARIB (i–l) and AMZN (m–p). Panels are made with 115 715 total number of trajectories impacting either one of receptor regions. The contoured regions denote the area with a concentration of trajectories above 50.

particles being removed by dry deposition process, in addition to the increased likelihood of being intercepted by precipitation.[86]

Trajectories reaching AMZN from December–February have a more uniform distribution with peak number of trajectories taking between 200 to 250 hours to travel (Fig. 3a); however, the number of trajectories taking longer than 250 hours is also notable. On the other hand, trajectories reaching US-CARIB from June to August show a skewed distribution with peak number of trajectories occurring between 240 and 280 hours (Fig. 3c). The average travel time of trajectories is also summarized in Table S2.† Comparing the two peak seasons, the total number of trajectories taking less than 200 hours to travel is considerably higher during the AMZN peak season (10 468 *versus* 3997, Fig. 3a), which implies a higher probability of survival for the co-transported microorganisms. Additionally, the two datasets were analyzed *via* a Student's *t*-test for the difference of the means and results indicate that summertime trajectories impacting the US-CARIB travel on average for a significantly longer period of time compared to wintertime AMZN trajectories with higher than 95% statistical confidence. However, it should be noted that a considerable portion of these trajectories intercept the ITCZ region where the carried dust is scavenged *via* wet deposition mechanisms. This removal rate is reportedly higher for winter time trajectories reaching the AMZN region.[91] It is also crucial to address the level of reliability in HYSPLIT trajectories, specifically over extended time and distances. We address this issue with further details in Section 3.4.

Shorter travel times for AMZN peak season trajectories can be partly attributed to the shorter distance between the Amazon and arid regions of northern African continent.[51] The winter time transport of dust aerosols to the Amazon is attributed to the southward movement of the ITCZ, which allows for transport of dust aerosols carried by the trade winds to the latitudes farther south.[24] However, the long-term variations in the large-scale circulation regime over the tropical north Atlantic can cause irregularities in the transport of dust aerosols across the

 © 2025 The Author(s). Published by the Royal Society of Chemistry

Open Access Article. Published on 23 December 2024. Downloaded on 11/2/2025 12:57:08 AM.
This article is licensed under a Creative Commons Attribution-NonCommercial 3.0 Unported Licence.

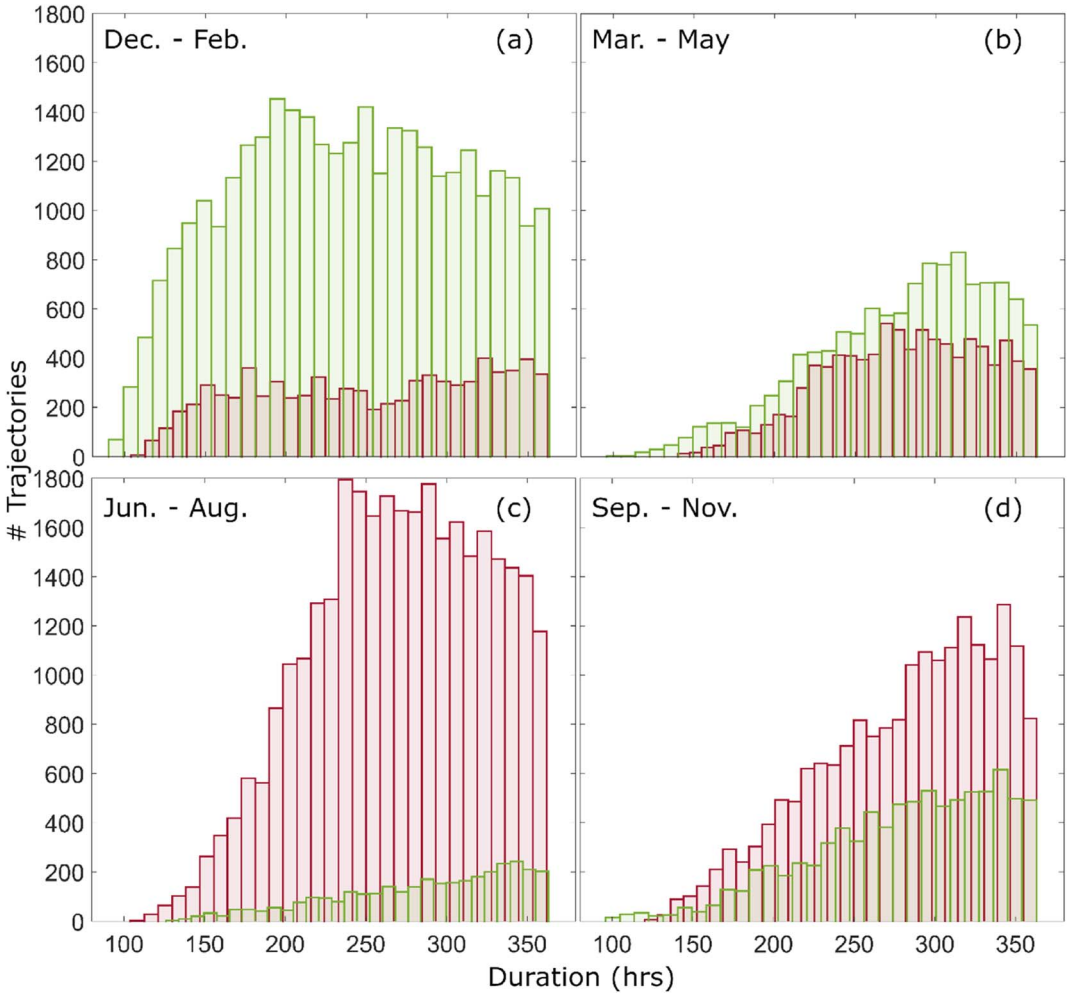


Fig. 3 Seasonal histograms of travel duration for trajectories reaching the US-CARIB (red), and AMZN (green) during December–February (a), March–May (b), June–August (c), and September–November (d). Histograms are made with a total number of 124 677 trajectories, including 8962 trajectories that are accounted for both sub-domains.

Atlantic. Examples of such interactions would be an estimated impact from widespread deforestation over tropics on increased dust transportation *via* weakening of the Hadley cell.[92] Irregularities in dust emission over African sources is another parameter impacting dust transport to the Amazon. As an example, separate analysis revealed a connection between the seasonal amount of rainfall in the Sahel region and the amount of seasonally emitted dust.[93,94]

From December to February, trajectories reaching the US-CARIB travel at time scales similar to the AMZN trajectories while the mean travel time from June to August is higher for trajectories reaching the AMZN. Relatively longer mean travel time of the summer trajectories impacting the AMZN sub-domain can be explained by differences observed in the transport regime of such trajectories, which closely follows the established seasonal variation in transport patterns of African dust plumes driven by Harmattan winds during the winter and transitioning into the Saharan air layer (SAL) in summer.[19] In a relevant study and over an 8 years period of 1995–2002, during July–October, Dunion[95] reported an average wind velocity of 5 m s$^{-1}$ for trajectories described as moist and tropical, arriving at the Caribbean majorly in the direction of easterly trade winds. These trajectories demonstrate characteristics similar to those impacting the AMZN sub-domain in the current study. In the same study, trajectories described as Saharan air layer travel considerably faster, with an average wind velocity of 9 m s$^{-1}$. This is also evident from the seasonally averaged flow of the wind over the tropical Atlantic Ocean and the neighboring regions (Fig. S2 and S3†), both within and above the marine boundary layer. Focusing on the free troposphere (Fig. S3†), a strong corridor of wind forms at around 20° N, mainly during the season of June–August and partly extends into the season of September–November. This corridor extends from the western coast of Africa to the Caribbean and acts as an atmospheric bridge, transporting plumes of dust between the two regions. From March to May, the observed pattern for travel times is somewhat similar to June–August. However, outside the peak seasons the number of trajectories is considerably lower. From September to November, trajectories of both receptor regions

Open Access Article. Published on 23 December 2024. Downloaded on 11/2/2025 12:57:08 AM.
This article is licensed under a Creative Commons Attribution-NonCommercial 3.0 Unported Licence.

demonstrate similar travel times with a higher number of trajectories reaching US-CARIB.

### 3.2. Dust emission activities

To isolate North African dust sources and any associated microorganisms contributing to each receptor region, composite maps of dust emission activities were made by summing up total seasonal dust emission activity associated with trajectories impacting each receptor region, as shown in Fig. 4. Focusing only on emissions capable of reaching our receptor regions on the western coasts of the Atlantic, the new seasonal maps differ from the mean seasonal dust emission maps (compare Fig. 4 and Fig. S4†). Note that maps in Fig. 4 are generated for the regions nominated as seasonally significant sources of dust emission (hashed areas in Fig. S4†) and not the entirety of Northern African regions. That is the reason for the sharp contrast observed between adjacent pixels in some regions. The new sets of maps in Fig. 4 are made for 124 677 trajectories that have impacted either one of receptor sub-domains including 8962 trajectories that are counted for both. On the maps, most emission regions were clustered around the west and southern regions of the North African continent with minimal impact from the north and eastern sources, even though on seasonal analysis, north and eastern regions

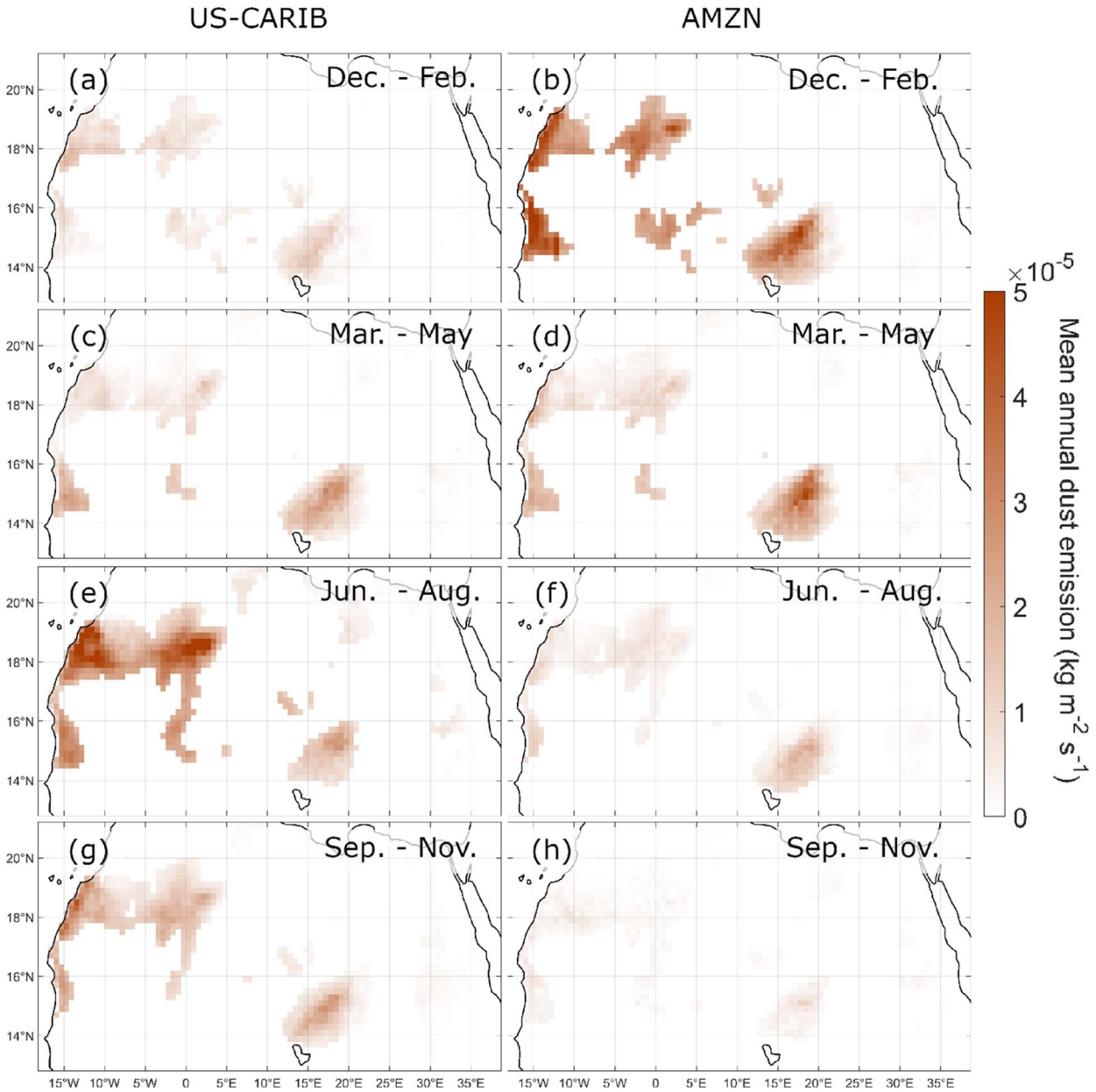


Fig. 4 Total seasonal dust emissions associated with trajectories impacting US-CARIB (a, c, e, and g) and AMZN (b, d, f, and h) based on the NASA Modern-Era Retrospective analysis for Research and Applications, Version 2 (MERRA-2) dust emission dataset. Seasonal number of trajectories impacting each receptor sub-domain are summarized in Table 1, including 8962 trajectories accounted for both sub-domains.

 © 2025 The Author(s). Published by the Royal Society of Chemistry

Open Access Article. Published on 23 December 2024. Downloaded on 11/2/2025 12:57:08 AM.
This article is licensed under a Creative Commons Attribution-NonCommercial 3.0 Unported Licence.

demonstrated statistically significant dust emission levels based on a gamma distribution fitted to the long-term daily emission values of each pixel. Such composite maps of seasonal dust emissions are also presented in ref. 93 study of dust variability over Northern Africa with spatial patterns following Fig. 4, even though timespans selected as seasons are slightly different from this study.

Seasonal variations in total amount of dust that reach each receptor region can be partly explained by the seasonal variations in dust emission activity of nominated hotspots and partly by seasonal variations in general flow of wind over the tropical Atlantic Ocean. The role of boundary layer wind flow in activity of dust sources is most evident over the Bodélé depression where average flow of wind in the boundary layer is highest during the December–February season (Fig. S2a†), in accordance with the highest emission observed (Fig. S3a†). During the boreal winter season, such strong Harmattan winds are combined with the strong flow of wind over the tropical Atlantic Ocean at around the equator (Fig. S3a†) that leads to the greatest dust transport activity from the Bodélé and sources at western regions to the AMZN receptor area. For the US-CARIB region, the June to August emissions stand out from the other seasons. This would be no surprise as it is also the season during which the majority of trajectories reach this receptor region. Similarly, during the December–February season when the majority of trajectories reach AMZN, total dust emission associated with these trajectories is more pronounced, compared to the rest of the year (Fig. 4b). At vertical levels representing the boundary layer processes, high emission rates are expected for dust sources located at western regions of Africa almost all year long (four panels of Fig. S2†). However, it is only during the June–August season that strong westward flow of wind in free troposphere bridges the west African emissions to the US-CARIB areas (Fig. S3c†).

Comparing the June–August season of US-CARIB with December–February season for AMZN enables us to better understand which North African sources have the highest impact on each receptor region. In summary, results indicate that for the US-CARIB region and during the high dust season (June–August), the majority of emissions come from sources located on the western half of North Africa. This follows the results reported by Gläser *et al.*,[51] Kumar *et al.*,[49] Pourmand *et al.*,[48] and Yu *et al.*,[11,91] even though the extent of the receptor regions slightly differs between the studies. Winter was observed as the peak season for dust transport to AMZN with a great impact perceived from Bodélé depression emissions, in accordance with previous studies.[96,97]

### 3.3. Ambient meteorological conditions along the trajectories

The diversity and concentration of viable microorganisms arriving at each receptor region is linked to the amount of dust traveled as well as the meteorological parameters along the trajectory.[98] The erythemal part of the solar ultraviolet (UV) radiation, which mainly consists of UV-B (280–315 nm) is one of the main factors reducing the viability of microorganisms from the upper atmosphere, especially ones with lower resistance to UV radiation.[99] Desiccation and extreme temperatures in the upper levels of troposphere may also reduce the viability of microorganisms during transit.[100] Consequently, we examined the mean solar radiation flux, ambient temperature, and RH along the trajectories in an effort to highlight the differences observed in meteorological conditions of different seasons and discuss the potential impact they have on the viability of microorganisms during transport from emission sources to receptor regions. Additionally, we analyzed the accumulated amount of precipitation perceived by each trajectory from above, as a measure of dust aerosol removal due to wet deposition.

Fig. 5 compares the histograms of average solar radiation flux, ambient temperature, and RH along the trajectories for dust aerosols reaching US-CARIB during the June–August, and AMZN during the December–February season. Only the peak seasons with the highest number of trajectories were compared to demonstrate the contrast between the two peak dust transfer seasons. Regardless of the region, trajectories receive higher and more uniform levels of mean solar radiation during the June to August season with an average of 370 W $m^{-2}$ for the US-CARIB region as compared to 294 W $m^{-2}$ for the AMZN region (Fig. 5a and b). Additionally, the spatial distribution of trajectories colored with average received solar radiation flux is depicted in Fig. 6 (panel a and b) for the same seasons. The area denoted with contours of 1, 5, and 10 on each panel of Fig. 6 denotes the pixels with 1, 5, and 10 percent of total seasonal dust emissions passing above them, respectively. In other words, the majority of total seasonal dust emission passes through the denoted corridors. For the AMZN, the average received solar radiation flux is higher for those trajectories passing from lower latitudes yet trajectories reaching the US-CARIB region demonstrate a more uniform distribution, latitudinally. Within the HYSPLIT model, downward solar radiation is calculated as the amount of solar radiation reaching the Earth's surface for each grid point, based on the cloud coverage and solar elevation angle.[63] The seasonal shift in solar elevation angle explains the observed difference between boreal summer and winter. During summer, trajectories tend to travel with less latitudinal variations (5°–25° N) and with relatively consistent solar angles. In contrast, trajectories reaching the Amazon region span a wider latitudinal range (10° S–30° N), leading to greater variability in experienced solar elevation angle. Solar radiation levels reaching the Earth's surface might differ from those perceived by trajectories above the clouds, particularly when trajectories pass above the low-level cloud decks. However, the tropical Atlantic Ocean experiences minimal low-level cloud cover, and mainly in the form of disorganized cloud formations cells.[101]

Relying solely on average values would be an oversimplification of the impact from meteorological parameters, and the cumulative amount of time a trajectory receives a certain level of solar radiation is another key parameter impacting the longevity of microorganisms. Panels (a) and (b) in Fig. 7 demonstrate the histograms of the cumulated solar radiation fluxes in the form of solar dose by summing up hourly

Open Access Article. Published on 23 December 2024. Downloaded on 11/2/2025 12:57:08 AM.
This article is licensed under a Creative Commons Attribution-NonCommercial 3.0 Unported Licence.

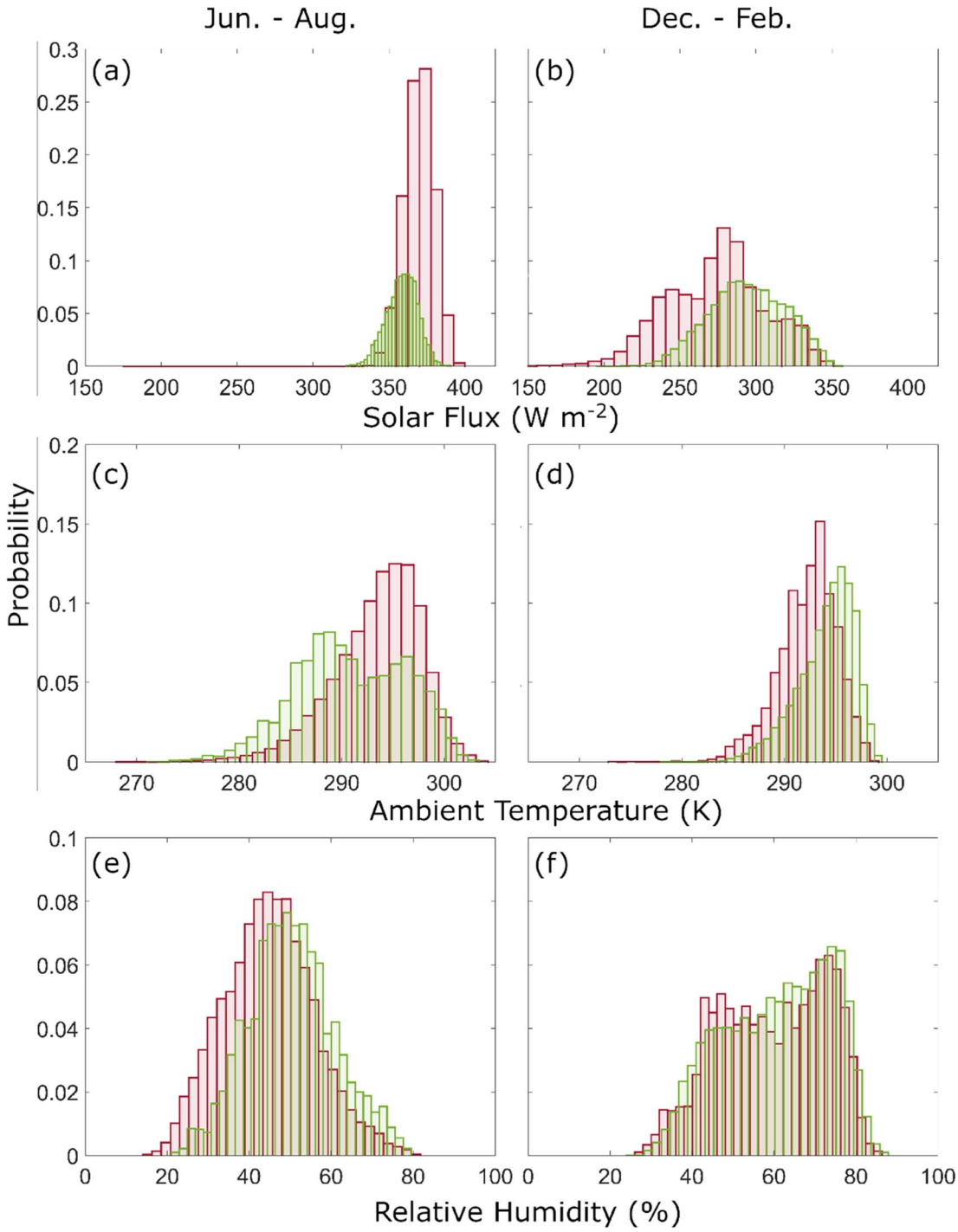


Fig. 5 Probability histograms of average conditions along the trajectories impacting US-CARIB (red) and AMZN (green) for solar radiation flux (a and b), ambient temperature (c and d), RH (e and f). Only peak seasons of June–August for US-CARIB and December–February for AMZN are compared.

averages. Considering the duration of travel time, histograms are now more dispersed and trajectories are impacted by a wider range of solar dose. Still, solar doses are higher on average for both receptor regions during the June to August peak season and trajectories demonstrate a more distinct peak in histogram of solar doses perceived by summertime trajectories.

The erythemal UV portion of the total atmospheric irradiance is dependent on geographic location, time of the year, and total ozone column concentration in the atmosphere and is discussed in detail by Utrillas *et al.*[102] Following their results, we assume 0.02% of total atmospheric irradiance as erythemal UV radiation. Using this conversion rate, dust trajectories are estimated to be exposed to UV radiation levels ranging from 20–100

 © 2025 The Author(s). Published by the Royal Society of Chemistry

Open Access Article. Published on 23 December 2024. Downloaded on 11/2/2025 12:57:08 AM.
This article is licensed under a Creative Commons Attribution-NonCommercial 3.0 Unported Licence.

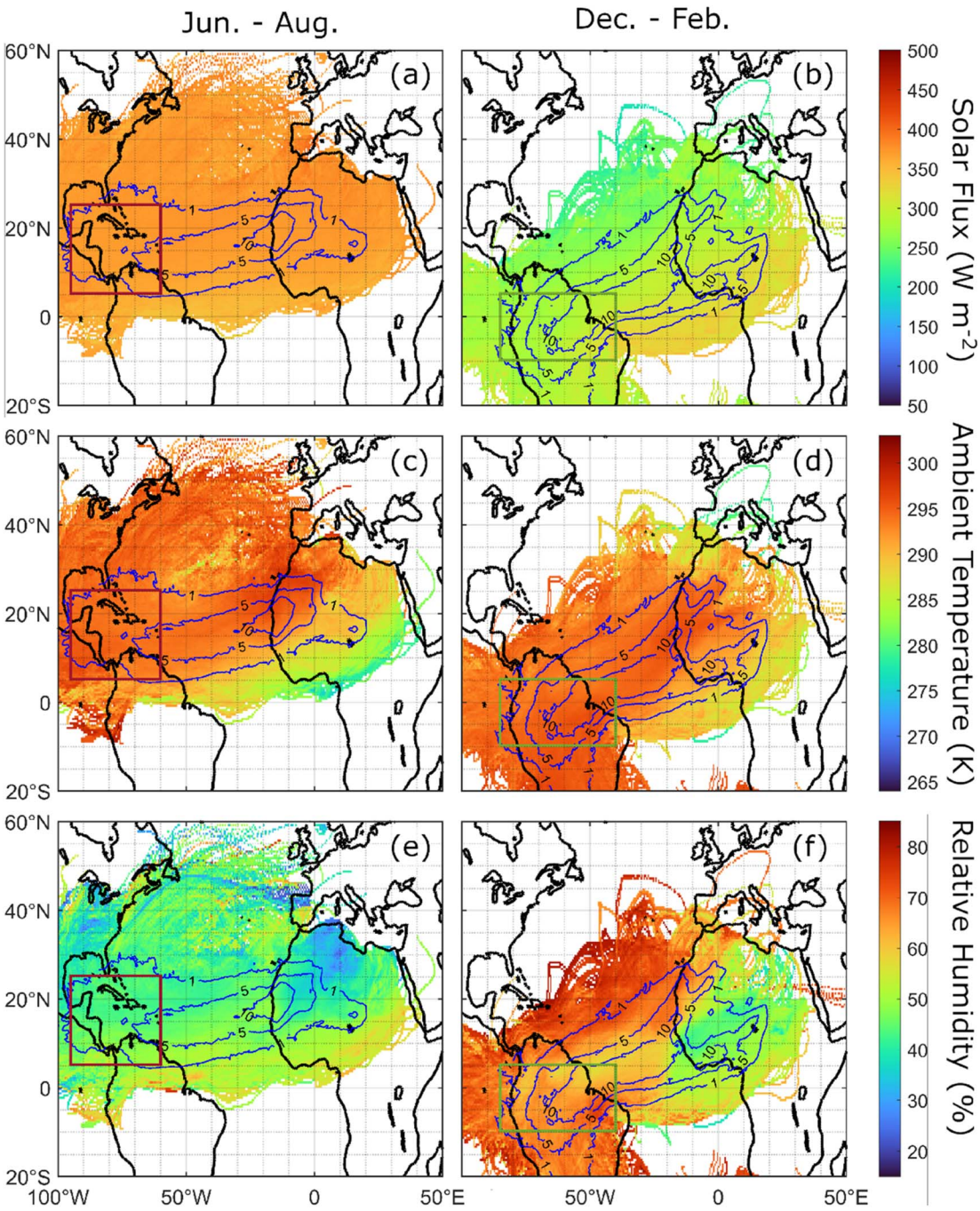


Fig. 6 Average parameters along the trajectories impacting US-CARIB during the June–August season (a, c, and e) and AMZN during the December–February season (b, d, and f). Areas denoted by blue contour lines represent pixels having at least 1, 5, and 10 percent of the total dust emission for trajectories passing above them, respectively.

kJ m$^{-2}$. To provide some context, it is reported that UV radiation levels of around 40 J m$^{-2}$ are capable of a one log decrease in concentration of microorganisms in a single stage decay model, which decreases the chance of survival for non-UV resistant microorganisms to extremely low levels.[82] However, it should be noted that these results are obtained in the lab environment and certain UV resisting strains of microorganisms are capable of surviving up to 2 kJ m$^{-2}$ of UV radiation with minimal decay and no negative correlation with UV concentration, which increases their chance of survival in extreme atmospheric conditions.[99] The established positive increase in the concentration of viable microorganisms from samples of long-range transported dust is suggestive of co-transported microorganisms' capability to survive the extreme atmospheric environment, within dense dust plumes[103] and in spite of extremely high doses of erythemal UV radiation. Survival of

Open Access Article. Published on 23 December 2024. Downloaded on 11/2/2025 12:57:08 AM.
This article is licensed under a Creative Commons Attribution-NonCommercial 3.0 Unported Licence.

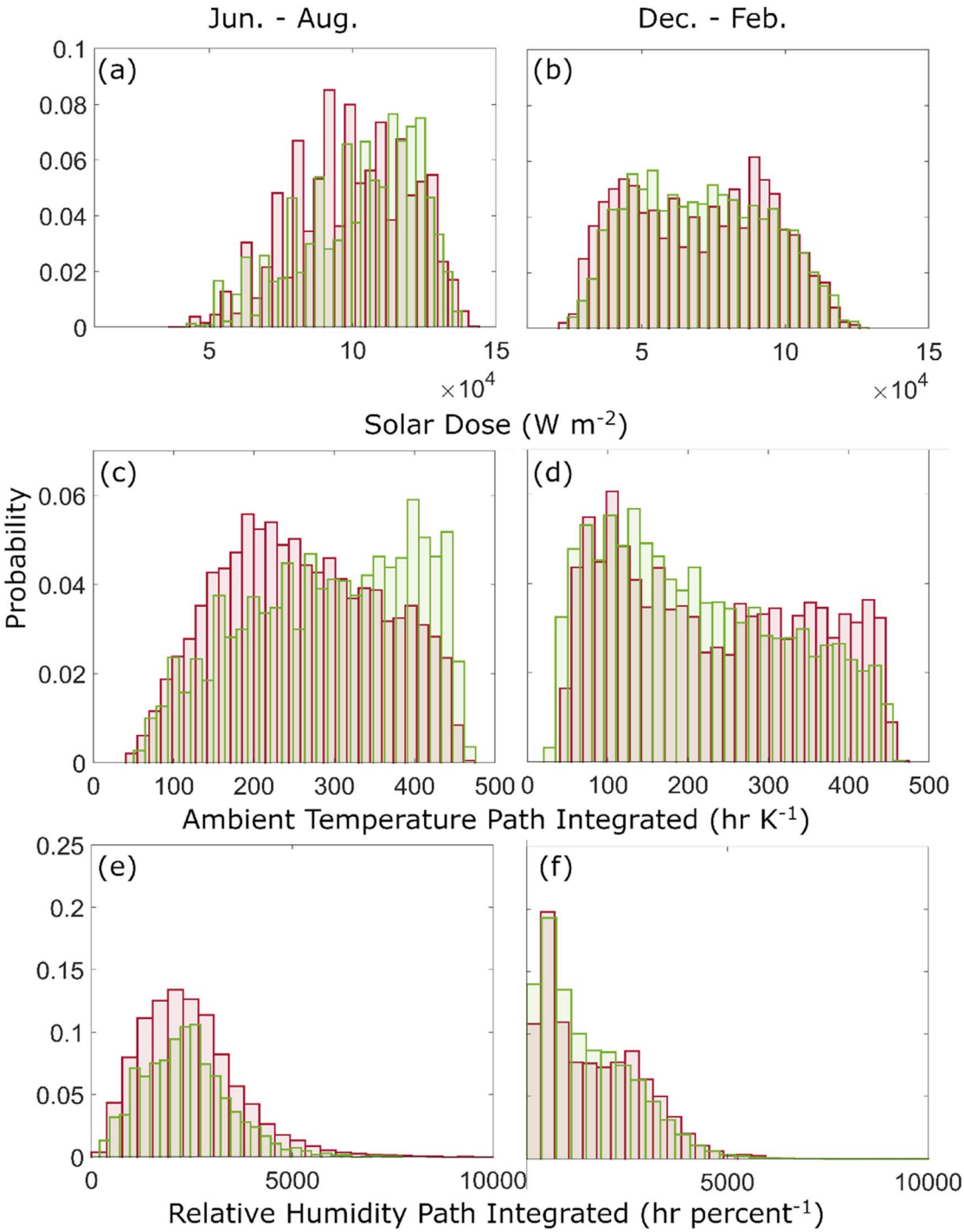


Fig. 7 Histograms of path-integrated meteorological parameters along the trajectories impacting US-CARIB (blue) and AMZN (orange) for solar dose flux (a and b), ambient temperature (c and d), and RH (e and f). Only peak seasons of June–August for US-CARIB and December–February for AMZN are compared. A higher path integrated value of temperature or RH reflects a lower temperature or RH level impacting the aerosols for a longer period of time.

microorganisms during extreme atmospheric conditions can be partly explained by attenuation of UV radiation by dust aerosols at higher levels of atmosphere[104] or microorganisms being shielded from UV radiation within the cracks and crevasses of inorganic dust aerosols.[38] Furthermore, adapting UV resistant abilities such as forming cell clumps or aggregates can increase microorganisms' UV survivability,[99] which is a common feature among microorganism taxa that are usually found in desert soils.[105] It is hypothesized that similar DNA repair characteristics, which make a phenotype resistant to UV radiation, will also increase the ability to survive other environmental stressors such

 © 2025 The Author(s). Published by the Royal Society of Chemistry

Open Access Article. Published on 23 December 2024. Downloaded on 11/2/2025 12:57:08 AM.
This article is licensed under a Creative Commons Attribution-NonCommercial 3.0 Unported Licence.

as desiccation,[106] and therefore, UV resistance can be considered the key parameter in survivability of microbes in the atmosphere.

Next, we compared the average ambient temperature along the trajectories for the same seasons and regions. When comparing trajectories reaching the peak receptor regions of each season, no discernible difference can be noted with an average of 293.5 K for US-CARIB from June to August as compared to 294.1 K for AMZN from December to February. However, summertime AMZN trajectories experience higher mean temperatures which can be due to traveling from more southern latitudes during the boreal summer. Moving from the most southern latitudes of this corridor up to the highest ones, a difference of around 5 K is noted for the trajectories during both seasons but in the middle of the corridor where the trajectories are more concentrated, average ambient temperature is the highest and most uniform.

Compared to histograms of average conditions, histograms of path-integrated ambient temperatures (see eqn (1)) are more dispersed, mainly due to variable travel time of trajectories (Fig. 7, panel c and d). The peak value appears around 150–250 h $K^{-1}$ for trajectories reaching US-CARIB from July to August and from 50–150 h $K^{-1}$ for AMZN trajectories from December to February. Mean values do not exhibit a significant difference, hence, the observed difference of path-integrated ambient temperature is mainly due to different travel times of trajectories reaching each receptor region. For atmospheric microorganisms, there is evidence in support of high temperature (27 °C on average) as a suitable condition and lower temperature (23 °C on average) as a limiting factor for the survivability of microorganisms.[107] As lower mean path integrated ambient temperatures represent higher temperatures endured for a longer time, transport condition is more suitable for survivability of microorganisms transported to AMZN between December–February. Nevertheless, Zhai *et al.*[108] reviewed results from numerous studies of temperature impacts on the survivability of microorganisms in the atmosphere and reported some contradicting results, and thus, concluded that the range of atmospheric conditions and type of microorganisms should be taken into consideration.

Finally, the RH along the trajectories is compared for the peak seasons with an average of 45 ± 11% for trajectories reaching US-CARIB during the June–August season and 61 ± 13% for AMZN during the December–February season. Compared to US-CARIB, the distribution of AMZN trajectories is more skewed with more trajectories experiencing a higher RH (Fig. 5e and f) and a bimodal distribution. It was discussed earlier that the majority of the summer-time trajectories travel above the boundary layer, while the majority of winter time trajectories travel at much lower altitudes and within the marine boundary layer (see panels k and m in Fig. 2). As a result, the difference between the averages of RH for the bulk of trajectories in two peak seasons can be attributed to the sharp difference in RH observed above and within the marine boundary layer.[109] Additionally, higher levels of RH are expected for winter time trajectories due to positioning of ITCZ and proximity of trajectories to this region.

During the December–February season, a striking divergence can be seen in the histograms of RH for trajectories reaching the AMZN region (Fig. 5e and f). This is characterized by a bimodal distribution, which is attributed to an increased number of trajectories originating from Bodélé and spending more time traversing arid regions. Among the meteorological parameters examined, RH exhibits the most significant contrast between land and ocean, which is to be expected as the ocean plays a significant role in determining RH levels. This is evident on panel f in Fig. 6 where wintertime trajectories sourced from the Bodélé depression that spend a longer time over continental Africa, experience lower mean levels of RH compared to the rest of the trajectories. However, wintertime trajectories reaching the AMZN overall experience higher RH levels.

RH also has a crucial role in the removal of aerosols by increasing their size through hygroscopic growth and accelerating the rate of dry deposition. This is due to the fact that even a small increase in particle size can significantly boost their fall velocity by up to 10 times, leading to a faster rate of dry deposition.[110] Based on some modeling analysis, this increase can be even higher for particles with a diameter in the range of 0.1–10 μm, which includes great portion of dust aerosols.[111] Based on the literature, the RH level of 98% was assumed as a criterion above which the size of particles increases significantly due to hygroscopicity.[112,113] Even though aerosol hygroscopic growth can occur at RH levels around 70%, such high levels of RH are selected due to the hydrophobic nature of Saharan dust relative to more hydrophilic aerosols commonly found in the atmosphere.[114] In addition to the dry deposition, wet scavenging of dust aerosols during precipitation periods is another mechanism for their removal from the atmosphere. Within the HYSPLIT model, precipitation is reported as the cumulative rainfall observed at ground level at each step of the analysis.[115] Considering that over the Atlantic Ocean, the majority of precipitation is derived from clouds positioned at altitudes exceeding 4700 meters above sea level,[116] consequently, nearly all trajectories are influenced by the recorded precipitation data provided by the HYSPLIT model. Accordingly, nearly all trajectories travel outside the high-altitude clouds and are not impacted by high RH levels inside the cloud layer. This motivates the analysis of the cumulative time aerosols spent under the influence of RH levels above 98% and as a function of total accumulated precipitation along the trajectories. For context, Dadashazar *et al.*[77] calculated a 53% reduction in the ratio of $PM_{2.5}$ relative to background CO levels when comparing >13.5 mm accumulated precipitation along trajectories from North America to Bermuda *versus* trajectories with <0.9 mm accumulated precipitation. Hilario *et al.*[78] demonstrated that a higher accumulated precipitation along trajectories was associated with much lower aerosol concentrations during transport over the West Pacific. The impact of precipitation along the trajectories was also studied along trajectories originating from the South American continent and moving toward the Pacific Ocean.[80] They concluded that trajectories with accumulated precipitation above 50 mm demonstrate distinctive characteristics of wet scavenging on plumes. Yu *et al.*[91] discussed that in contrary to previous studies, the Bodélé

Open Access Article. Published on 23 December 2024. Downloaded on 11/2/2025 12:57:08 AM.
This article is licensed under a Creative Commons Attribution-NonCommercial 3.0 Unported Licence.

depression plays a little role in contributing to the dust load over the Amazon and a greater contribution comes from northwestern sources like the El Djouf region. In their study, they highlighted the impact from wet deposition due to precipitation as one of the main removal mechanisms of dust emitted from the Bodélé depression. However, the possibility of dust transport is not ruled out entirely and the proven record of African dust samples over the Amazon and the Caribbean basin, makes the long-range transport of viable microorganisms a possibility. Caution should be taken as in this study; dust aerosols are analyzed for their role in transport of viable microorganisms. Unlike nutrients that should be continuously carried in considerable amounts to leave a measurable impact on the receptor site, even a few instances of viable microorganism transport can leave a notable impact on the biota of the receptor regions.

Fig. 8 compares histograms of accumulated precipitation along the trajectories impacting each sub-domain during the June–August and December–February seasons. Average accumulated precipitation along the trajectories was 13.69 and 18.16 mm for US-CARIB and AMZN, respectively. Higher mean precipitation values observed for AMZN trajectories can be attributed in part to a higher proportion of trajectories passing in close proximity to the ITCZ during the peak season for the Amazon (Fig. 2). This proximity increases the likelihood of these trajectories intersecting with precipitating clouds. However, by isolating trajectories to a region encompassing solely the Bodélé depression from 15°–19° latitude and 15.5°–19.5° longitude, the average accumulated precipitation along trajectories does not undergo a notable change, which suggests that based on the current methodology, there is not a statistically significant difference between precipitation perceived by trajectories initiated from Bodélé, as compared to the rest of the trajectories during the winter season.

In contrast, US-CARIB trajectories follow paths at more northern latitudes during the boreal summer, placing them farther from the ITCZ summertime location. The established lower mean travel altitude[20,21] for trajectories during the boreal winter is another parameter that increases the endured RH levels by wintertime trajectories and hence, increases their chance of removal. It is worth mentioning that two main mechanisms of convective cold pools and the nocturnal low-level jets account for more than 80% of dust emission incidents over the arid regions of Africa.[117] Both mechanisms meteorologically drive the dust emission over the warm and dry continental North Africa during the summer, where extremely low levels of moisture exist in the atmosphere.[118] As a dust layer reaches the west African coast, it slides above the cool marine air mass and is lifted to higher altitudes[119] which gives the trajectories little to no chance of enduring high RH levels before leaving the continental regions.

Field measurements also confirm that there is a significant rise in RH levels within the boundary layer compared to drier conditions in the free troposphere, with an increase of up to three times.[120] Another explanation of higher precipitation along the wintertime trajectories would be the location of a high-precipitation band across the Atlantic Ocean. Summertime precipitation across the tropical Atlantic Ocean happens between 0° N–15° N (ref. 121) and shifts southward, between 10° S–10° N during the winter.[122] In both seasons, the greater portion of precipitation occurs in close proximity to the coast of the South American Continent. As the majority of summertime trajectories travel above and parallel to the summer band of precipitation (Fig. 6), a lower portion of them are intercepted and washed out by heavy precipitation while on the other hand, wintertime trajectories travel within high-precipitation zones and hence, endure a higher precipitation along the trajectories.

Around 14% of AMZN trajectories exhibit accumulated precipitation levels higher than 30 mm, compared to around 8% percent of US-CARIB trajectories. We did the same analysis for the duration each trajectory spends in RH levels above 98% (not shown in figure). Of the trajectories impacting AMZN, around 4.7% spend at least one hour in such conditions. The

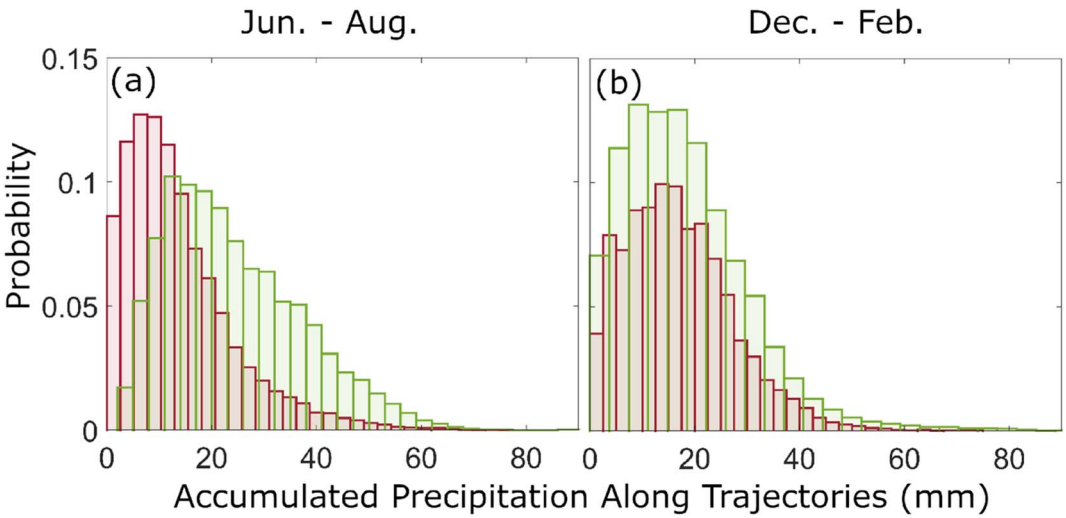


Fig. 8 Histograms of accumulated precipitation along the trajectories for seasons of (a) June–August and (b) December–February. Blue and orange denote trajectories impacting US-CARIB and AMZN, respectively.

 © 2025 The Author(s). Published by the Royal Society of Chemistry

Open Access Article. Published on 23 December 2024. Downloaded on 11/2/2025 12:57:08 AM.
This article is licensed under a Creative Commons Attribution-NonCommercial 3.0 Unported Licence.

analogous analysis for US-CARIB trajectories revealed significantly lower values (<0.2%). Overall, the combined impact of ambient moisture levels, either in form of precipitation or high RH levels is not strong enough to totally eliminate the airborne dust from the atmosphere. This is also evident from the presence of dust during the rainy seasons at receptor sites.[22,59] However, the role of wet deposition mechanisms in removal of dust should be considered when assessing the amount of dust reaching each receptor sub-domain.

### 3.4. Implications for the transport of microorganisms

The effect of meteorological factors on the survival of airborne microorganisms has been widely studied.[123] Bacteria, virus, and fungi have different characteristics that help them overcome adverse atmospheric conditions (*e.g.*, extreme temperatures, low water and nutrient availability, high solar radiation, desiccation). Cellular characteristics, such as rigid cell walls in Gram-positive bacteria, make microorganisms more resistant to damage. Also, spore-forming microorganisms, like fungi and some bacteria, can survive under adverse circumstances, because they are able to stop or decrease their metabolism.

Traditionally in studies of airborne microorganisms, temperature and RH have been considered to have a positive impact on microbial abundance.[124–126] However, this seems to be partially true only for culture-based studies. Next-generation sequencing analyses of airborne communities have not detected such correlation,[127–130] and some even have described how bacterial richness may increase under low temperature conditions.[131] Upon closer look, meteorological factors, such as temperature and RH may have a specific influence on different groups of microorganisms. For instance, Park *et al.*[132] found a negative correlation between temperature and the phylum Proteobacteria, while this correlation was positive with the Firmicutes and Bacteroidetes phyla. Some authors consider that at higher temperatures, the solar radiation usually increases as well, which can lead to a decrease in the microbial survival rates due to DNA damage.[126]

A notable example is that of Waters *et al.*,[133] where metagenomes from trans-Atlantic airborne dust samples were compared to data from the Chad region, speculated to be the source of the dust. Despite the metagenomes of airborne samples not closely clustering with the speculated origin of the dust, they exhibited similarities irrespective of the temporal distances of collection, ranging from months to a year. The conclusion drawn is that atmospheric dust samples develop similarities due to atmospheric processes. Additionally, the study suggests that the interaction between airborne samples and the oceanic microbiome could be another significant factor influencing the atmospheric microbiome over the Atlantic Ocean, leading to numerous shared traits among the samples.

By considering the similarities between atmospheric dust samples and how the microbial airborne community may change due to factors such as continuous mixing with atmospheric aerosols and deposition during their transport, specific protective mechanisms unique to each microbe, and specific characteristics of each dust event (*e.g.*, particle sizes, dust plume altitude, and amount of dust), results from the current study may benefit prediction of the effects of the environmental factors and chance of survival for specific groups of microorganisms.

## 4. Conclusions

In this study, we integrated the NASA MERRA-2 dust emission scheme with the NOAA HYSPLIT forward trajectory analysis to study spatiotemporal characteristics of more than half a million trajectories carrying dust aerosols across the Atlantic during a 14 year period (2008–2021). We followed the dust transport pathway from its emission sources over Sahara and Sahel regions in North Africa until reaching receptor areas as far as the southeast U.S., Caribbean, and Amazon. Along the transport paths, we studied the meteorological conditions endured by dust aerosols with a main focus on parameters impacting concentration, diversity, and longevity of co-transported microorganisms. Results are suggestive of the following conclusions:

- Modeling results closely follow the established seasonal pattern of dust emission and transport from northern African sources and across the tropical Atlantic Ocean[12–15,47,59,118,134,135] with the majority of westward, dust-carrying trajectories entering the southeastern regions of the United States and the Caribbean basin during the summer season (June–August). In winter (December–February), the majority of trajectories enter the Amazon basin. Other seasons of the year serve as transitory times when the total number of westward trajectories are split between the two sub-domains.

- Similarly, the vertical structure of travel paths closely follow the seasonal variations observed from CALIOP's vertically resolved aerosol concentration per season and receptor region[17,19–21] with significant differences between the two seasons. During summer (June–August), trajectories traverse the Atlantic at a significantly higher altitude compared to winter (December–February) trajectories. Summer trajectories mainly travel above the marine boundary layer and demonstrate characteristics mentioned for the Saharan air layer which, is described to reach higher altitudes, above the cooler moist marine boundary layer air mass upon leaving the North African continent[136] at around 10° N–25° N. In addition to the preceding observations, another altitudinal characteristic of the dry and warm Saharan air layer which is closely reproduced by the current modeling results is a travel altitude between 1–5 km near the coast of Africa that can occasionally reach altitudes of 5–6 km (ref. 137) and descend to 0–3 km as trajectories approach the Caribbean basin.[21] In contrast, winter trajectories spend a greater portion of their travel time within the marine boundary layer in a relatively cooler and moist ambient environment.

- Analysis of dust emission incidents associated with trajectories suggests that during the summer time, the majority of dust intruding the US-CARIB basin is emitted from sources located on the western side of arid regions of northern Africa. However, other source regions such as the Bodélé depression play a role as well. During the winter time and for trajectories impacting the AMZN sub-domain, the Bodélé depression emits the greater portion of the intruding dust but source regions are

Open Access Article. Published on 23 December 2024. Downloaded on 11/2/2025 12:57:08 AM.
This article is licensed under a Creative Commons Attribution-NonCommercial 3.0 Unported Licence.

not clustered as clearly as they are during the summer. Distinct emission sources during each peak season suggest different taxa of microorganisms being co-transported with dust aerosols. Additionally, a higher diversity of microorganisms is expected during the winter solely based on a more diverse source base.

- Long-term analysis of dust emitting regions during the peak seasons suggests an interannual oscillation in the equivalent center of emissions for the winter time between the western regions and the Bodélé depression. However, during summer, such spatial variation is not as profound and emission sources are more clustered. Accordingly, a higher interannual variation is expected for the taxa of microorganisms being co-transported with dust aerosols during the winter.

- Trajectories take an average of 270 hours during the summer and 239 hours during the winter to reach receptor subdomains in the Americas. These timeframes are shorter than the 13 day timescales cited for the transport of dust aerosols to the world's most remote areas.[39–41] Based solely on atmospheric travel times, microorganisms co-transported to the AMZN subdomain have a higher likelihood of survival.

- During summer, trajectories endure significantly higher and more uniform levels of solar UV radiation when compared to the winter season. Endured RH is also lower on average for the summer time trajectories intruding the US-CARIB subdomain. A bimodal distribution is observed in the histogram of the mean RH endured by wintertime trajectories impacting the AMZN sub-domain. Overall, ambient meteorological conditions are less suitable for the survivability of co-transported microorganisms during summertime.

- Periods of intense precipitation and high RH contribute to the removal of dust aerosols from the atmosphere, however, the total number of trajectories impacted by such conditions constitute no more than 14% of trajectories reaching AMZN sub-domain in winter and 8% trajectories reaching the US-CARIB sub-domain in summer.

The present study is a part of the ongoing NASA Microbes in Trans-Atlantic Dust (MITAD) field campaign, which aims to investigate microbial long-range transport and survival in dust plumes *via* an interdisciplinary approach that integrates multiplatform observations such as remote sensing, reanalysis, and atmospheric simulation data with microbiological analysis performed on a series of dust samples, collected at multiple locations across the Atlantic Ocean. Future studies will focus on specific taxa of airborne microorganisms detected in actual dust samples and the correlation between their concentration, diversity, longevity, and environmental conditions in the atmosphere.

## Data availability

MERRA-2 dataset used in preparation of this manuscript can be accessed from (**https://doi.org/10.5067/HM00OHQBHKTP**) and NCEP/NCAR meteorology files used for HYSPLIT trajectory analysis are stored in (**ftp://ftp.arl.noaa.gov/pub/archives/reanalysis**). NCEP-NCAR Reanalysis 1 data provided by the NOAA PSL, Boulder, Colorado, USA, from their website at **https://psl.noaa.gov**.

## Conflicts of interest

There are no conflicts to declare.

## Acknowledgements

This research is supported by the National Aeronautics and Space Administration (NASA) under Grant 80NSSC20K1532. AS and MRAH were supported by NASA Grant 80NSSC19K0442 for ACTIVATE, a NASA Earth Venture Suborbital-3 (EVS-3) investigation funded by NASA's Earth Science Division and managed through the Earth System Science Pathfinder Program Office. The authors acknowledge the NOAA Air Resources Laboratory (ARL) for the provision of the HYSPLIT transport and dispersion model accessible from the READY website (**http://ready.arl.noaa.gov**) and NOAA Physical Sciences Laboratory (PSL) for the provision of the NCEP-NCAR Reanalysis 1 accessible from the PSL website (**https://www.psl.noaa.gov**) used in this work.

## References

1 J. F. Kok, A. A. Adebiyi, S. Albani, Y. Balkanski, R. Checa-Garcia, M. Chin, P. R. Colarco, D. S. Hamilton, Y. Huang and A. Ito, Improved representation of the global dust cycle using observational constraints on dust properties and abundance, *Atmos. Chem. Phys. Discuss.*, 2020, **2020**, 1–45.
2 S. Kinne, M. Schulz, C. Textor, S. Guibert, Y. Balkanski, S. E. Bauer, T. Berntsen, T. Berglen, O. Boucher and M. Chin, An AeroCom initial assessment–optical properties in aerosol component modules of global models, *Atmos. Chem. Phys.*, 2006, **6**, 1815–1834.
3 Y. Shao, *Physics and Modelling of Wind Erosion*, Springer, 2008.
4 J. F. Kok, A. A. Adebiyi, S. Albani, Y. Balkanski, R. Checa-Garcia, M. Chin, P. R. Colarco, D. S. Hamilton, Y. Huang and A. Ito, Contribution of the world's main dust source regions to the global cycle of desert dust, *Atmos. Chem. Phys.*, 2021, **21**, 8169–8193.
5 L. Schütz, Long range transport of desert dust with special emphasis on the Sahara, *Ann. N. Y. Acad. Sci.*, 1980, **338**, 515–532.
6 G. A. d'Almeida, A model for Saharan dust transport, *J. Appl. Meteorol. Climatol.*, 1986, **25**, 903–916.
7 A. M. Adams, J. M. Prospero and C. Zhang, CALIPSO-derived three-dimensional structure of aerosol over the Atlantic Basin and adjacent continents, *J. Clim.*, 2012, **25**, 6862–6879.
8 P. Ginoux, J. M. Prospero, T. E. Gill, N. C. Hsu and M. Zhao, Global-scale attribution of anthropogenic and natural dust sources and their emission rates based on MODIS Deep Blue aerosol products, *Rev. Geophys.*, 2012, **50**(3), RG3005.

 © 2025 The Author(s). Published by the Royal Society of Chemistry

Open Access Article. Published on 23 December 2024. Downloaded on 11/2/2025 12:57:08 AM.
This article is licensed under a Creative Commons Attribution-NonCommercial 3.0 Unported Licence.

9 Y. Kaufman, I. Koren, L. Remer, D. Tanré, P. Ginoux and S. Fan, Dust transport and deposition observed from the Terra-Moderate Resolution Imaging Spectroradiometer (MODIS) spacecraft over the Atlantic Ocean, *J. Geophys. Res.:Atmos.*, 2005, **110**(D10), 10–12.

10 Z. Liu, A. Omar, M. Vaughan, J. Hair, C. Kittaka, Y. Hu, K. Powell, C. Trepte, D. Winker and C. Hostetler, CALIPSO lidar observations of the optical properties of Saharan dust: A case study of long-range transport, *J. Geophys. Res.:Atmos.*, 2008, **113**(D10), DOI: 10.1029/2007JD008878.

11 H. Yu, Q. Tan, L. Zhou, Y. Zhou, H. Bian, M. Chin, C. L. Ryder, R. C. Levy, Y. Pradhan and Y. Shi, Observation and modeling of the historic "Godzilla" African dust intrusion into the Caribbean Basin and the southern US in June 2020, *Atmos. Chem. Phys.*, 2021, **21**, 12359–12383.

12 J. M. Prospero, P. Ginoux, O. Torres, S. E. Nicholson and T. E. Gill, Environmental characterization of global sources of atmospheric soil dust identified with the Nimbus 7 Total Ozone Mapping Spectrometer (TOMS) absorbing aerosol product, *Rev. Geophys.*, 2002, **40**, 2.

13 R. Washington, M. Todd, N. J. Middleton and A. S. Goudie, Dust-storm source areas determined by the total ozone monitoring spectrometer and surface observations, *Ann. Am. Assoc. Geogr.*, 2003, **93**, 297–313.

14 S. Engelstaedter, I. Tegen and R. Washington, North African dust emissions and transport, *Earth-Sci. Rev.*, 2006, **79**, 73–100.

15 I. Ashpole and R. Washington, Intraseasonal variability and atmospheric controls on daily dust occurrence frequency over the central and western Sahara during the boreal summer, *J. Geophys. Res.:Atmos.*, 2013, **118**, 12915–12926.

16 D. Liu, Y. Wang, Z. Wang and J. Zhou, The three-dimensional structure of transatlantic African dust transport: A new perspective from CALIPSO LIDAR measurements, *Adv. Meteorol.*, 2012, **2012**, 850704.

17 D. Liu, Z. Wang, Z. Liu, D. Winker and C. Trepte, A height resolved global view of dust aerosols from the first year CALIPSO lidar measurements, *J. Geophys. Res.:Atmos.*, 2008, **113**(D16), DOI: 10.1029/2007JD009776.

18 K. Schepanski, I. Tegen, B. Laurent, B. Heinold and A. Macke, A new Saharan dust source activation frequency map derived from MSG-SEVIRI IR-channels, *Geophys. Res. Lett.*, 2007, **34**, L18803.

19 P. Knippertz and M. C. Todd, Mineral dust aerosols over the Sahara: Meteorological controls on emission and transport and implications for modeling, *Rev. Geophys.*, 2012, **50**(1), DOI: 10.1029/2011RG000362.

20 Y. Ben-Ami, I. Koren and O. Altaratz, Patterns of North African dust transport over the Atlantic: winter vs. summer, based on CALIPSO first year data, *Atmos. Chem. Phys.*, 2009, **9**, 7867–7875.

21 C. Tsamalis, A. Chédin, J. Pelon and V. Capelle, The seasonal vertical distribution of the Saharan Air Layer and its modulation by the wind, *Atmos. Chem. Phys.*, 2013, **13**, 11235–11257.

22 J. Prospero, R. Glaccum and R. Nees, Atmospheric transport of soil dust from Africa to South America, *Nature*, 1981, **289**, 570–572.

23 E. Jung, B. Albrecht, J. M. Prospero, H. H. Jonsson and S. M. Kreidenweis, Vertical structure of aerosols, temperature, and moisture associated with an intense African dust event observed over the eastern Caribbean, *J. Geophys. Res.:Atmos.*, 2013, **118**, 4623–4643.

24 R. Jaenicke, Abundance of cellular material and proteins in the atmosphere, *Science*, 2005, **308**, 73.

25 E. Mayol, J. M. Arrieta, M. A. Jiménez, A. Martínez-Asensio, N. Garcias-Bonet, J. Dachs, B. González-Gaya, S.-J. Royer, V. M. Benítez-Barrios and E. Fraile-Nuez, Long-range transport of airborne microbes over the global tropical and subtropical ocean, *Nat. Commun.*, 2017, **8**, 201.

26 Y. Shi, S. Lai, Y. Liu, S. Gromov and Y. Zhang, Fungal aerosol diversity over the northern South China Sea: the influence of land and ocean, *J. Geophys. Res.:Atmos.*, 2022, **127**, e2021JD035213.

27 S. M. Burrows, W. Elbert, M. Lawrence and U. Pöschl, Bacteria in the global atmosphere–Part 1: Review and synthesis of literature data for different ecosystems, *Atmos. Chem. Phys.*, 2009, **9**, 9263–9280.

28 S. Burrows, T. Butler, P. Jöckel, H. Tost, A. Kerkweg, U. Pöschl and M. Lawrence, Bacteria in the global atmosphere–Part 2: Modeling of emissions and transport between different ecosystems, *Atmos. Chem. Phys.*, 2009, **9**, 9281–9297.

29 C. A. Kellogg and D. W. Griffin, Aerobiology and the global transport of desert dust, *Trends Ecol. Evol.*, 2006, **21**, 638–644.

30 P. H. Gregory, The Leeuwenhoek Lecture 1970 Airborne microbes: their significance and distribution, *Proc. R. Soc. London, Ser. B*, 1971, **177**, 469–483.

31 A. A. Gorbushina, R. Kort, A. Schulte, D. Lazarus, B. Schnetger, H. J. Brumsack, W. J. Broughton and J. Favet, Life in Darwin's dust: intercontinental transport and survival of microbes in the nineteenth century, *Environ. Microbiol.*, 2007, **9**, 2911–2922.

32 J. K. Brown and M. S. Hovmøller, Aerial dispersal of pathogens on the global and continental scales and its impact on plant disease, *Science*, 2002, **297**, 537–541.

33 A. Giongo, J. Favet, A. Lapanje, K. A. Gano, S. Kennedy, A. G. Davis-Richardson, C. Brown, A. Beck, W. G. Farmerie and A. Cattaneo, Microbial hitchhikers on intercontinental dust: high-throughput sequencing to catalogue microbes in small sand samples, *Aerobiologia*, 2013, **29**, 71–84.

34 C. Gonzalez-Martin, N. Teigell-Perez, B. Valladares and D. W. Griffin, The global dispersion of pathogenic microorganisms by dust storms and its relevance to agriculture, *Adv. Agron.*, 2014, **127**, 1–41.

35 J. Favet, A. Lapanje, A. Giongo, S. Kennedy, Y.-Y. Aung, A. Cattaneo, A. G. Davis-Richardson, C. T. Brown, R. Kort and H.-J. Brumsack, Microbial hitchhikers on intercontinental dust: catching a lift in Chad, *ISME J.*, 2013, **7**, 850–867.

Open Access Article. Published on 23 December 2024. Downloaded on 11/2/2025 12:57:08 AM.
This article is licensed under a Creative Commons Attribution-NonCommercial 3.0 Unported Licence.

36 N. Yamaguchi, T. Ichijo, A. Sakotani, T. Baba and M. Nasu, Global dispersion of bacterial cells on Asian dust, *Sci. Rep.*, 2012, **2**, 525.
37 C. Rodriguez-Gomez, C. Ramirez-Romero, F. Cordoba, G. B. Raga, E. Salinas, L. Martinez, I. Rosas, E. T. Quintana, L. A. Maldonado and D. Rosas, Characterization of culturable airborne microorganisms in the Yucatan Peninsula, *Atmos. Environ.*, 2020, **223**, 117183.
38 D. W. Griffin, V. H. Garrison, J. R. Herman and E. A. Shinn, African desert dust in the Caribbean atmosphere: microbiology and public health, *Aerobiologia*, 2001, **17**, 203–213.
39 Y. Iwasaka, H. Minoura and K. Nagaya, The transport and spacial scale of Asian dust-storm clouds: a case study of the dust-storm event of April 1979, *Tellus B*, 1983, **35**, 189–196.
40 I. Uno, K. Eguchi, K. Yumimoto, T. Takemura, A. Shimizu, M. Uematsu, Z. Liu, Z. Wang, Y. Hara and N. Sugimoto, Asian dust transported one full circuit around the globe, *Nat. Geosci.*, 2009, **2**, 557–560.
41 S. Zhang, S. Hou, X. Ma, D. Qin and T. Chen, Culturable bacteria in Himalayan glacial ice in response to atmospheric circulation, *Biogeosciences*, 2007, **4**, 1–9.
42 D. Gat, Y. Mazar, E. Cytryn and Y. Rudich, Origin-dependent variations in the atmospheric microbiome community in Eastern Mediterranean dust storms, *Environ. Sci. Technol.*, 2017, **51**, 6709–6718.
43 Y. Mazar, E. Cytryn, Y. Erel and Y. Rudich, Effect of dust storms on the atmospheric microbiome in the Eastern Mediterranean, *Environ. Sci. Technol.*, 2016, **50**, 4194–4202.
44 E. Rahav, A. Paytan, C.-T. Chien, G. Ovadia, T. Katz and B. Herut, The impact of atmospheric dry deposition associated microbes on the southeastern mediterranean sea surface water following an intense dust storm, *Front. Mar. Sci.*, 2016, **3**, 127.
45 E. A. Shinn, D. W. Griffin and D. B. Seba, Atmospheric transport of mold spores in clouds of desert dust, *Arch. Environ. Occup. Health*, 2003, **58**, 498.
46 K. Hara and D. Zhang, Bacterial abundance and viability in long-range transported dust, *Atmos. Environ.*, 2012, **47**, 20–25.
47 J. M. Prospero, A. C. Delany, A. C. Delany and T. N. Carlson, The discovery of African dust transport to the Western Hemisphere and the Saharan air layer: A history, *Bull. Am. Meteorol. Soc.*, 2021, 1–53.
48 A. Pourmand, J. M. Prospero and A. Sharifi, Geochemical fingerprinting of trans-Atlantic African dust based on radiogenic Sr-Nd-Hf isotopes and rare earth element anomalies, *Geology*, 2014, **42**, 675–678.
49 A. Kumar, W. Abouchami, S. Galer, S. P. Singh, K. Fomba, J. Prospero and M. O. Andreae, Seasonal radiogenic isotopic variability of the African dust outflow to the tropical Atlantic Ocean and across to the Caribbean, *Earth Planet. Sci. Lett.*, 2018, **487**, 94–105.
50 A. E. Barkley, J. M. Prospero, N. Mahowald, D. S. Hamilton, K. J. Popendorf, A. M. Oehlert, A. Pourmand, A. Gatineau, K. Panechou-Pulcherie and P. Blackwelder, African biomass burning is a substantial source of phosphorus deposition to the Amazon, Tropical Atlantic Ocean, and Southern Ocean, *Proc. Natl. Acad. Sci. U. S. A.*, 2019, **116**, 16216–16221.
51 G. Gläser, H. Wernli, A. Kerkweg and F. Teubler, The transatlantic dust transport from North Africa to the Americas—Its characteristics and source regions, *J. Geophys. Res.:Atmos.*, 2015, **120**, 11231–11252.
52 A. C. Schuerger, D. J. Smith, D. W. Griffin, D. A. Jaffe, B. Wawrik, S. M. Burrows, B. C. Christner, C. Gonzalez-Martin, E. K. Lipp and D. G. Schmale III, Science questions and knowledge gaps to study microbial transport and survival in Asian and African dust plumes reaching North America, *Aerobiologia*, 2018, **34**, 425–435.
53 A. Grini, G. Myhre, C. S. Zender and I. S. Isaksen, Model simulations of dust sources and transport in the global atmosphere: Effects of soil erodibility and wind speed variability, *J. Geophys. Res.:Atmos.*, 2005, **110**(D2), DOI: 10.1029/2004JD005037.
54 K. Schepanski, B. Heinold and I. Tegen, Harmattan, Saharan heat low, and West African monsoon circulation: modulations on the Saharan dust outflow towards the North Atlantic, *Atmos. Chem. Phys.*, 2017, **17**, 10223–10243.
55 R. Gelaro, W. McCarty, M. J. Suárez, R. Todling, A. Molod, L. Takacs, C. A. Randles, A. Darmenov, M. G. Bosilovich and R. Reichle, The modern-era retrospective analysis for research and applications, version 2 (MERRA-2), *J. Clim.*, 2017, **30**, 5419–5454.
56 P. Ginoux, M. Chin, I. Tegen, J. M. Prospero, B. Holben, O. Dubovik and S. J. Lin, Sources and distributions of dust aerosols simulated with the GOCART model, *J. Geophys. Res.:Atmos.*, 2001, **106**, 20255–20273.
57 B. Marticorena and G. Bergametti, Modeling the atmospheric dust cycle: 1. Design of a soil-derived dust emission scheme, *J. Geophys. Res.:Atmos.*, 1995, **100**, 16415–16430.
58 J. Meng, Y. Huang, D. M. Leung, L. Li, A. A. Adebiyi, C. L. Ryder, N. M. Mahowald and J. F. Kok, Improved parameterization for the size distribution of emitted dust aerosols reduces model underestimation of super coarse dust, *Geophys. Res. Lett.*, 2022, **49**, e2021GL097287.
59 J. M. Prospero, F. X. Collard, J. Molinié and A. Jeannot, Characterizing the annual cycle of African dust transport to the Caribbean Basin and South America and its impact on the environment and air quality, *Global Biogeochem. Cycles*, 2014, **28**, 757–773.
60 G. Bergametti, A.-L. Dutot, P. Buat-Menard, R. Losno and E. Remoudaki, Seasonal variability of the elemental composition of atmospheric aerosol particles over the northwestern Mediterranean, *Tellus B*, 1989, **41**, 353–361.
61 P. N. Polymenakou, M. Mandalakis, E. G. Stephanou and A. Tselepides, Particle size distribution of airborne microorganisms and pathogens during an intense African dust event in the eastern Mediterranean, *Environ. Health Perspect.*, 2008, **116**, 292–296.

 © 2025 The Author(s). Published by the Royal Society of Chemistry

Open Access Article. Published on 23 December 2024. Downloaded on 11/2/2025 12:57:08 AM.
This article is licensed under a Creative Commons Attribution-NonCommercial 3.0 Unported Licence.

62 S. Fiedler, K. Schepanski, P. Knippertz, B. Heinold and I. Tegen, How important are atmospheric depressions and mobile cyclones for emitting mineral dust aerosol in North Africa?, *Atmos. Chem. Phys.*, 2014, **14**, 8983–9000.
63 R. R. Draxler and G. Hess, Description of the HYSPLIT4 modeling system, *NOAA technical Memorandum ERL ARL*, 1997, p. 224.
64 G. Rolph, A. Stein and B. Stunder, Real-time environmental applications and display system: READY, *Environ. Model. Softw.*, 2017, **95**, 210–228.
65 A. F. Stein, R. R. Draxler, G. D. Rolph, B. J. Stunder, M. D. Cohen and F. Ngan, NOAA's HYSPLIT atmospheric transport and dispersion modeling system, *Bull. Am. Meteorol. Soc.*, 2015, **96**, 2059–2077.
66 P. D. Neff and N. A. Bertler, Trajectory modeling of modern dust transport to the Southern Ocean and Antarctica, *J. Geophys. Res.:Atmos.*, 2015, **120**, 9303–9322.
67 R. Swap, M. Garstang, S. Greco, R. Talbot and P. Kållberg, Saharan dust in the Amazon Basin, *Tellus B*, 1992, **44**, 133–149.
68 Y. Ben-Ami, I. Koren, Y. Rudich, P. Artaxo, S. Martin and M. Andreae, Transport of North African dust from the Bodélé depression to the Amazon Basin: a case study, *Atmos. Chem. Phys.*, 2010, **10**, 7533–7544.
69 H. McGowan and A. Clark, Identification of dust transport pathways from Lake Eyre, Australia using Hysplit, *Atmos. Environ.*, 2008, **42**, 6915–6925.
70 S. S. Abdalmogith and R. M. Harrison, The use of trajectory cluster analysis to examine the long-range transport of secondary inorganic aerosol in the UK, *Atmos. Environ.*, 2005, **39**, 6686–6695.
71 O. Doherty, N. Riemer and S. Hameed, Control of Saharan mineral dust transport to Barbados in winter by the Intertropical Convergence Zone over West Africa, *J. Geophys. Res.:Atmos.*, 2012, **117**(D19), 19117.
72 J. Huang, C. Zhang and J. M. Prospero, African dust outbreaks: A satellite perspective of temporal and spatial variability over the tropical Atlantic Ocean, *J. Geophys. Res.:Atmos.*, 2010, **115**(D5), DOI: 10.1029/2009JD012516.
73 E. Kalnay, M. Kanamitsu, R. Kistler, W. Collins, D. Deaven, L. Gandin, M. Iredell, S. Saha, G. White and J. Woollen, in *Renewable Energy*, Routledge, 2018, pp. Vol1_146-Vol141_194.
74 T. M. Trzeciak, L. Garcia-Carreras and J. H. Marsham, Cross-Saharan transport of water vapor via recycled cold pool outflows from moist convection, *Geophys. Res. Lett.*, 2017, **44**, 1554–1563.
75 D. H. Bromwich and R. L. Fogt, Strong trends in the skill of the ERA-40 and NCEP–NCAR reanalyses in the high and midlatitudes of the Southern Hemisphere, 1958–2001, *J. Clim.*, 2004, **17**, 4603–4619.
76 G. Wotawa and M. B. Kalinowski, Evaluation of the operational IDC ATM products by comparing HYSPLIT BA, FA and OMEGA FOR during Level 4 events in Scandinavia, *Proceedings of the Informal Workshop on Meteorological Modelling in Support of CTBT Verification*, 2000, pp. 4–6.
77 H. Dadashazar, M. Alipanah, M. R. A. Hilario, E. Crosbie, S. Kirschler, H. Liu, R. H. Moore, A. J. Peters, A. J. Scarino and M. Shook, Aerosol responses to precipitation along North American air trajectories arriving at Bermuda, *Atmos. Chem. Phys.*, 2021, **21**, 16121–16141.
78 M. R. A. Hilario, E. Crosbie, M. Shook, J. S. Reid, M. O. L. Cambaliza, J. B. B. Simpas, L. Ziemba, J. P. DiGangi, G. S. Diskin and P. Nguyen, Measurement report: Long-range transport patterns into the tropical northwest Pacific during the CAMP 2 Ex aircraft campaign: chemical composition, size distributions, and the impact of convection, *Atmos. Chem. Phys.*, 2021, **21**, 3777–3802.
79 H. E. Fuelberg, R. O. Loring Jr, M. V. Watson, M. Sinha, K. E. Pickering, A. M. Thompson, G. W. Sachse, D. R. Blake and M. R. Schoeberl, TRACE A trajectory intercomparison: 2. Isentropic and kinematic methods, *J. Geophys. Res.:Atmos.*, 1996, **101**, 23927–23939.
80 S. Freitag, A. Clarke, S. Howell, V. Kapustin, T. Campos, V. Brekhovskikh and J. Zhou, Combining airborne gas and aerosol measurements with HYSPLIT: a visualization tool for simultaneous evaluation of air mass history and back trajectory consistency, *Atmos. Meas. Tech.*, 2014, **7**, 107.
81 J. M. Harris, R. R. Draxler and S. J. Oltmans, Trajectory model sensitivity to differences in input data and vertical transport method, *J. Geophys. Res.:Atmos.*, 2005, **110**(D14), DOI: 10.1029/2004JD005750.
82 W. Kowalski, *Ultraviolet Germicidal Irradiation Handbook: UVGI for Air and Surface Disinfection*, Springer science & business media, 2010.
83 K. Schepanski, I. Tegen and A. Macke, Saharan dust transport and deposition towards the tropical northern Atlantic, *Atmos. Chem. Phys.*, 2009, **9**, 1173–1189.
84 I. Chiapello, C. Moulin and J. M. Prospero, Understanding the long-term variability of African dust transport across the Atlantic as recorded in both Barbados surface concentrations and large-scale Total Ozone Mapping Spectrometer (TOMS) optical thickness, *J. Geophys. Res.:Atmos.*, 2005, **110**(D18), D18S10.
85 J. S. Reid, D. L. Westphal, J. M. Livingston, D. L. Savoie, H. B. Maring, H. H. Jonsson, D. P. Eleuterio, J. E. Kinney and E. A. Reid, Dust vertical distribution in the Caribbean during the Puerto Rico Dust Experiment, *Geophys. Res. Lett.*, 2002, **29**, 55.
86 S. Engelstaedter, R. Washington and N. Mahowald, Impact of changes in atmospheric conditions in modulating summer dust concentration at Barbados: A back-trajectory analysis, *J. Geophys. Res.:Atmos.*, 2009, **114**(D17), DOI: 10.1029/2008JD011180.
87 N. A. Aalismail, D. K. Ngugi, R. Díaz-Rúa, I. Alam, M. Cusack and C. M. Duarte, Functional metagenomic analysis of dust-associated microbiomes above the Red Sea, *Sci. Rep.*, 2019, **9**, 13741.
88 X. Chen, D. Kumari and V. Achal, A review on airborne microbes: the characteristics of sources, pathogenicity and geography, *Atmosphere*, 2020, **11**, 919.

Open Access Article. Published on 23 December 2024. Downloaded on 11/2/2025 12:57:08 AM.
This article is licensed under a Creative Commons Attribution-NonCommercial 3.0 Unported Licence.

89 M. Kowalski and J. S. Pastuszka, Effect of ambient air temperature and solar radiation on changes in bacterial and fungal aerosols concentration in the urban environment, *Ann. Agric. Environ. Med.*, 2018, **25**, 259–261.
90 D. J. Smith, D. W. Griffin, R. D. McPeters, P. D. Ward and A. C. Schuerger, Microbial survival in the stratosphere and implications for global dispersal, *Aerobiologia*, 2011, **27**, 319–332.
91 Y. Yu, O. V. Kalashnikova, M. J. Garay, H. Lee, M. Notaro, J. R. Campbell, J. Marquis, P. Ginoux and G. S. Okin, Disproving the Bodélé depression as the primary source of dust fertilizing the Amazon Rainforest, *Geophys. Res. Lett.*, 2020, **47**, e2020GL088020.
92 Y. Li, J. T. Randerson, N. M. Mahowald and P. J. Lawrence, Deforestation strengthens atmospheric transport of mineral dust and phosphorus from North Africa to the Amazon, *J. Clim.*, 2021, **34**, 6087–6096.
93 N. Brooks and M. Legrand, Dust variability over northern Africa and rainfall in the Sahel, *Linking Climate Change to Land Surface Change*, 2000, pp. 1–25.
94 J. M. Prospero and P. J. Lamb, African droughts and dust transport to the Caribbean: Climate change implications, *Science*, 2003, **302**, 1024–1027.
95 J. P. Dunion, Rewriting the climatology of the tropical North Atlantic and Caribbean Sea atmosphere, *J. Clim.*, 2011, **24**, 893–908.
96 C. S. Bristow, K. A. Hudson-Edwards and A. Chappell, Fertilizing the Amazon and equatorial Atlantic with West African dust, *Geophys. Res. Lett.*, 2010, **37**(14), DOI: 10.1029/2010GL043486.
97 R. Washington, C. Bouet, G. Cautenet, E. Mackenzie, I. Ashpole, S. Engelstaedter, G. Lizcano, G. M. Henderson, K. Schepanski and I. Tegen, Dust as a tipping element: the Bodélé Depression, Chad, *Proc. Natl. Acad. Sci. U. S. A.*, 2009, **106**, 20564–20571.
98 J. M. Prospero, E. Blades, G. Mathison and R. Naidu, Interhemispheric transport of viable fungi and bacteria from Africa to the Caribbean with soil dust, *Aerobiologia*, 2005, **21**, 1–19.
99 Y. Yang, S. Itahashi, S.-i. Yokobori and A. Yamagishi, UV-resistant bacteria isolated from upper troposphere and lower stratosphere, *Biological Sciences in Space*, 2008, **22**, 18–25.
100 D. W. Griffin, Atmospheric movement of microorganisms in clouds of desert dust and implications for human health, *Clin. Microbiol. Rev.*, 2007, **20**, 459–477.
101 A. Muhlbauer, I. L. McCoy and R. Wood, Climatology of stratocumulus cloud morphologies: microphysical properties and radiative effects, *Atmos. Chem. Phys.*, 2014, **14**, 6695–6716.
102 M. Utrillas, M. Marín, A. Esteve, G. Salazar, H. Suárez, S. Gandía and J. Martínez-Lozano, Relationship between erythemal UV and broadband solar irradiation at high altitude in Northwestern Argentina, *Energy*, 2018, **162**, 136–147.
103 P. Schlesinger, Y. Mamane and I. Grishkan, Transport of microorganisms to Israel during Saharan dust events, *Aerobiologia*, 2006, **22**, 259–273.
104 J. Herman, N. Krotkov, E. Celarier, D. Larko and G. Labow, Distribution of UV radiation at the Earth's surface from TOMS-measured UV-backscattered radiances, *J. Geophys. Res.:Atmos.*, 1999, **104**, 12059–12076.
105 M. Musilova, G. Wright, J. M. Ward and L. R. Dartnell, Isolation of radiation-resistant bacteria from Mars analog Antarctic Dry Valleys by preselection, and the correlation between radiation and desiccation resistance, *Astrobiology*, 2015, **15**, 1076–1090.
106 F. A. Rainey, K. Ray, M. Ferreira, B. Z. Gatz, M. F. Nobre, D. Bagaley, B. A. Rash, M.-J. Park, A. M. Earl and N. C. Shank, Extensive diversity of ionizing-radiation-resistant bacteria recovered from Sonoran Desert soil and description of nine new species of the genus Deinococcus obtained from a single soil sample, *Appl. Environ. Microbiol.*, 2005, **71**, 5225–5235.
107 M. Almaguer, M.-J. Aira, F. J. Rodríguez-Rajo and T. I. Rojas, Temporal dynamics of airborne fungi in Havana (Cuba) during dry and rainy seasons: influence of meteorological parameters, *Int. J. Biometeorol.*, 2014, **58**, 1459–1470.
108 Y. Zhai, X. Li, T. Wang, B. Wang, C. Li and G. Zeng, A review on airborne microorganisms in particulate matters: Composition, characteristics and influence factors, *Environ. Int.*, 2018, **113**, 74–90.
109 V. Wulfmeyer and G. Feingold, On the relationship between relative humidity and particle backscattering coefficient in the marine boundary layer determined with differential absorption lidar, *J. Geophys. Res.:Atmos.*, 2000, **105**, 4729–4741.
110 R. Arimoto, R. Duce, B. Ray and U. Tomza, Dry deposition of trace elements to the western North Atlantic, *Global Biogeochem. Cycles*, 2003, **17**(1), DOI: 10.1029/2001GB001406.
111 S. Sengupta, S. Sengupta, C. K. Chanda and H. Saha, Modeling the effect of relative humidity and precipitation on photovoltaic dust accumulation processes, *IEEE J. Photovolt.*, 2021, **11**, 1069–1077.
112 R. M. Williams, A model for the dry deposition of particles to natural water surfaces, *Atmos. Environ.*, 1967, **1982**(16), 1933–1938.
113 K. Koehler, S. Kreidenweis, P. DeMott, M. Petters, A. Prenni and C. Carrico, Hygroscopicity and cloud droplet activation of mineral dust aerosol, *Geophys. Res. Lett.*, 2009, **36**(8), DOI: 10.1029/2009GL037348.
114 N. Kaaden, A. Massling, A. Schladitz, T. Müller, K. Kandler, L. Schütz, B. Weinzierl, A. Petzold, M. Tesche and S. Leinert, State of mixing, shape factor, number size distribution, and hygroscopic growth of the Saharan anthropogenic and mineral dust aerosol at Tinfou, Morocco, *Tellus B*, 2009, **61**, 51–63.
115 R. Draxler, HYSPLIT (Hybrid single-particle Lagrangian integrated trajectory) model, http://www.arl.noaa.gov/HYSPLIT.php, 2003.

 © 2025 The Author(s). Published by the Royal Society of Chemistry

Open Access Article. Published on 23 December 2024. Downloaded on 11/2/2025 12:57:08 AM.
This article is licensed under a Creative Commons Attribution-NonCommercial 3.0 Unported Licence.

116 J. M. Haynes and G. L. Stephens, Tropical oceanic cloudiness and the incidence of precipitation: Early results from CloudSat, *Geophys. Res. Lett.*, 2007, **34**(9), DOI: 10.1029/2007GL029335.

117 B. Heinold, P. Knippertz, J. Marsham, S. Fiedler, N. Dixon, K. Schepanski, B. Laurent and I. Tegen, The role of deep convection and nocturnal low-level jets for dust emission in summertime West Africa: Estimates from convection-permitting simulations, *J. Geophys. Res.:Atmos.*, 2013, **118**, 4385–4400.

118 I. Koren, Y. J. Kaufman, R. Washington, M. C. Todd, Y. Rudich, J. V. Martins and D. Rosenfeld, The Bodélé depression: a single spot in the Sahara that provides most of the mineral dust to the Amazon forest, *Environ. Res. Lett.*, 2006, **1**, 014005.

119 M. Van Der Does, P. Knippertz, P. Zschenderlein, R. Giles Harrison and J.-B. W. Stuut, The mysterious long-range transport of giant mineral dust particles, *Sci. Adv.*, 2018, **4**, eaau2768.

120 H. Maring, D. Savioe, M. Izaguirre, L. Custals and J. Reid, Vertical distributions of dust and sea-salt aerosols over Puerto Rico during PRIDE measured from a light aircraft, *J. Geophys. Res.:Atmos.*, 2003, **108**(D19), DOI: 10.1029/2002JD002544.

121 A. C. Siongco, C. Hohenegger and B. Stevens, Sensitivity of the summertime tropical Atlantic precipitation distribution to convective parameterization and model resolution in ECHAM6, *J. Geophys. Res.:Atmos.*, 2017, **122**, 2579–2594.

122 M. Barreiro, P. Chang and R. Saravanan, Variability of the South Atlantic convergence zone simulated by an atmospheric general circulation model, *J. Clim.*, 2002, **15**, 745–763.

123 J. W. Tang, The effect of environmental parameters on the survival of airborne infectious agents, *J. R. Soc. Interface*, 2009, **6**, S737–S746.

124 P. Mouli, S. Mohan and S. Reddy, Assessment of microbial(bacteria) Concentrations of ambient air at semi-arid urban region: Influence of meteorological factors, *Appl. Ecol. Environ. Res.*, 2005, **3**, 139–149.

125 R. M. Harrison, A. M. Jones, P. D. Biggins, N. Pomeroy, C. S. Cox, S. P. Kidd, J. L. Hobman, N. L. Brown and A. Beswick, Climate factors influencing bacterial count in background air samples, *Int. J. Biometeorol.*, 2005, **49**, 167–178.

126 Y. Sun, Y. Huang, S. Xu, J. Li, M. Yin and H. Tian, Seasonal variations in the characteristics of microbial community structure and diversity in atmospheric particulate matter from clean days and smoggy days in Beijing, *Microb. Ecol.*, 2022, **83**, 568–582.

127 R. M. Bowers, I. B. McCubbin, A. G. Hallar and N. Fierer, Seasonal variability in airborne bacterial communities at a high-elevation site, *Atmos. Environ.*, 2012, **50**, 41–49.

128 S.-K. Shin, J. Kim, S.-m. Ha, H.-S. Oh, J. Chun, J. Sohn and H. Yi, Metagenomic insights into the bioaerosols in the indoor and outdoor environments of childcare facilities, *PLoS One*, 2015, **10**, e0126960.

129 A. Núñez, A. M. García, D. A. Moreno and R. Guantes, Seasonal changes dominate long-term variability of the urban air microbiome across space and time, *Environ. Int.*, 2021, **150**, 106423.

130 Q. Zhen, Y. Deng, Y. Wang, X. Wang, H. Zhang, X. Sun and Z. Ouyang, Meteorological factors had more impact on airborne bacterial communities than air pollutants, *Sci. Total Environ.*, 2017, **601**, 703–712.

131 C. González-Martín, C. J. Pérez-González, E. González-Toril, F. J. Expósito, Á. Aguilera and J. P. Díaz, Airborne bacterial community composition according to their origin in Tenerife, Canary Islands, *Front. Microbiol.*, 2021, **12**, 732961.

132 E. H. Park, J. Heo, H. Kim and S.-M. Yi, The major chemical constituents of PM2. 5 and airborne bacterial community phyla in Beijing, Seoul, and Nagasaki, *Chemosphere*, 2020, **254**, 126870.

133 S. M. Waters, S. Purdue, R. Armstrong and Y. Detrés, Metagenomic investigation of African dust events in the Caribbean, *FEMS Microbiol. Lett.*, 2020, **367**, fnaa051.

134 R. Washington, M. C. Todd, S. Engelstaedter, S. Mbainayel and F. Mitchell, Dust and the low-level circulation over the Bodélé Depression, Chad: Observations from BoDEx 2005, *J. Geophys. Res.:Atmos.*, 2006, **111**(D3), DOI: 10.1029/2005JD006502.

135 J. M. Prospero, A. E. Barkley, C. J. Gaston, A. Gatineau, A. Campos y Sansano and K. Panechou, Characterizing and quantifying African dust transport and deposition to South America: Implications for the phosphorus budget in the Amazon Basin, *Global Biogeochem. Cycles*, 2020, **34**, e2020GB006536.

136 V. M. Karyampudi and T. N. Carlson, Analysis and numerical simulations of the Saharan air layer and its effect on easterly wave disturbances, *J. Atmos. Sci.*, 1988, **45**, 3102–3136.

137 V. M. Karyampudi, S. P. Palm, J. A. Reagen, H. Fang, W. B. Grant, R. M. Hoff, C. Moulin, H. F. Pierce, O. Torres and E. V. Browell, Validation of the Saharan dust plume conceptual model using lidar, Meteosat, and ECMWF data, *Bull. Am. Meteorol. Soc.*, 1999, **80**, 1045–1076.